Mixed convection and mass transfer in the stagnation point flow of second grade fluid adjacent to vertical surface

By

Muhammad Arshad Siddiqui

A Dissertation
Submitted in the Partial Fulfillment of the
Requirements for the Degree of
MASTER OF SCIENCE
In
MATHEMATICS

Supervised by

Dr. Tariq Javed

Department of Mathematics and Statistics
Faculty of Basic and Applied Sciences
International Islamic University, Islamabad
Pakistan
2011

_1_. Boundary layer

بسم الله الرحمن الرحيم
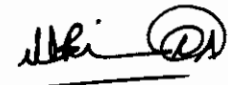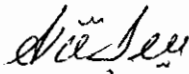
Certificate

Mixed convection and mass transfer in the stagnation point flow of second grade fluid adjacent to vertical surface

By

Muhammad Arshad Siddiqui

A DISSERTATION SUBMITTED IN THE PARTIAL FULFILLMENT OF THE REQUIREMENTS FOR THE DEGREE OF THE **MASTER OF SCIENCE in MATHEMATICS**

We accept this dissertation as conforming to the required standard.

1. _____ 23/12/11
   Prof. Dr. Tasawar Hayat
   (External Examiner)

2. _____
   Dr. Nasir Ali
   (Internal Examiner)

3. _____
   Dr. Tariq Javed
   (Supervisor)

4. _____
   Dr. Irshad Ahmad Arshad
   (Chairman)

Department of Mathematics and Statistics
Faculty of Basic and Applied Sciences
International Islamic University, Islamabad
Pakistan
2011

<u>Dedication</u>

I dedicate my research work of my **MS (Mathematics)** to my beloved mother **Jannat-un-Nisa** (Late), whose clear vision and outstanding personality gave me an insight to the understanding of myself and the world.

Acknowledgement

First and foremost, I am thankful to Almighty Allah, who created us, taught us everything we know, provided us with the health, knowledge and Intelligence to explore this world.

The task of my **MS (Mathematics)** research was not an easy thing. When I started to work on my research problem, I felt it to be very hectic and painstaking. But then some of my dear and near ones, made this heavy task much lighter and enjoyable for me. First of all I am very thankful to my supervisor **Dr. Tariq Javed** whose assistance put me to the right track of research. Then I am very thankful to my father **G.M. Siddiqui,** who appreciated me for my efforts. Then I would like to show my gratitude to my elder brothers, **Abdul Razzaq, Fazal Razzaq, Mohammad Akhtar** and **Mohammad Asif** respectively as they always encouraged me throughout my research work. Then the role of my eldest sister, **Ayesha Bibi** cannot be denied as she has a big hand in my studies generally and in my higher studies specifically. Of course I cannot forget to mention that I owe a lot to the pray of my sweet sisters. The role my friends, **Dr. Ahmed Zeeshan, Rashid Ali, Nouman Ijaz, Sheraz Khalid** and **Touseef** is also worthy to be mentioned over here whose moral support and encouragement helped me a lot to fulfill my research work. If the help and appreciation of all the above mentioned people had not been there, then perhaps I had not been able to achieve my goal. So once again, I show my gratitude to all of them.

Muhammad Arshad Siddiqui
December 23, 2011

DECLARATION

I hereby declare that this thesis, neither as a whole nor as a part thereof, has been copied out from any source. It is further declared that I have prepared this thesis entirely on the basis of my personal efforts made under the sincere guidance of my supervisor. No portion of the work, presented in this thesis, has been submitted in the support of any application for any degree or qualification of this or any other institute of learning.

Signature: _____

MUHAMMAD ARSHAD SIDDIQUI

MS Mathematics

Reg. No. 33-FBAS/MSMA/S09

Department of Mathematics and Statistics

Faculty of Basic and Applied Sciences

International Islamic University Isalamabad

Pakistan

Preface

Boundary layer flows of incompressible fluid over a stretched surface has many industrial applications such as aerodynamic extrusion of plastic sheets, boundary layer flows along liquid films in condensation processes, cooling of a metallic plate in cooling bath and in glass and polymer industries. The investigations regarding boundary layer flows were performed by many researchers such as Sakiadis [1], Crane [2], Banks [3], Grubka and Bobba [4], Banks and Zaturska [5], Erickson et al [6] for the impermeable plate and Gupta and Gupta [7], Chen and Char [8], Ali [9], Chaudhary et al [10], Elbashbeshy [11], Magyari and Keller [12] for the permeable plate. In his paper, Banks [3] gave solution by using numerical approach and was unable to give dual solution due to high sensitivity of numerical scheme he used. Furthermore, his solution was without velocity reversed flows. Goldstein [13] gave the physical meanings of negative stretching velocity corresponding to the backward boundary layer. As pointed out by Magyari and Keller [14] and Liao and Pop [15], the considered problem is mathematically equivalent to the steady free convection flow over a vertical semi-infinite plate which is embedded in a fluid saturated porous medium described by Cheng and Minkowycz's equation [16,17] after employing the homotopy analysis method [18-20]. Recently Pop and Na [21] reported multiple solutions for MHD flows over a stretched permeable surface. Zaturska and Banks [22] found multiple solutions for Blasius boundary layer flows. Magyari et al [23] found multiple solutions of boundary layer flows over a moving plane surface. However Magyari et al [24] found multiple solution of the considered problem at $\beta = -1/2$. After that Liao produced a new branch of solutions in his paper [25] and to the best of our knowledge, dual solutions of the boundary flows over a stretched impermeable wall for $\beta > 1$ have not been reported earlier.

The theory of non-Newtonian fluids has become a field of very active research for last few decades as this class of fluids represents many industrial fluids as well. Several authors have considered the viscoelastic fluids whose constitutive equations are based on the assumption of gradually fading memory [26-29]. The steady incompressible flow of a viscoelastic fluid in the region of a two-dimensional stagnation point flow has been studied by Beard and Walter [30] and Garg and Rajagopal [31]. The equation of motion of viscoelastic fluids are one order higher than available boundary conditions. In order to overcome this difficulty Beard and Walter [30] used perturbation technique. However Garg and Rajagopal [31] tackled this difficulty by assuming one extra boundary condition at infinity and used quasilinearization along with orthonormalization. This method is further used by Seshadri et al [32] to investigate unsteady three-dimensional stagnation point flow of a viscoelastic fluid. Ramachandran [33] and Lok [34] discussed the mixed convection in stagnation point flow adjacent to vertical surface of Newtonian and micro-polar fluids respectively. Hiemenz [35] considered the flow in the neighborhood of stagnation line with characteristic irrespective of the shape of the body. Hayat et al. [36] discussed the mixed convection in the stagnation point flow adjacent to a vertical surface of a viscoelastic fluid. The dissertation is arranged as follows:

Chapter 1 includes some prerequisites and basic definitions for the convenience and better understanding of the reader. The concepts of Chapter 2 are based on the work of S.J. Liao [25]. All the results are reproduced successfully. In Chapter 3 we reproduced the work of Hayat et al [36] and extended this analysis by considering the mass-transfer in the stagnation point flow adjacent to vertical surface.

Contents

3

Chapter 1

Preliminaries

1.1 Introduction

In this chapter, some basic definitions, concepts of various types of fluids and basic equations which govern the flow are described. The basic idea of homotopy, homotopy analysis method (HAM) and homotopy-Padé approximation are also explained in this chapter.

1.2 Basic definitions

1.2.1 Flow

In the presence of different forces, a material like liquid or gases goes under deformation. In many cases this deformation is change of position of its particles and it continuously increases without limit, this phenomenon is known as flow.

1.2.2 Fluid

A fluid is a substance that flows under the action of shearing forces.

1.2.3 Fluid mechanics

Fluid mechanics is the branch of Engineering and physical sciences that deals with the forces on fluids and their actions. Fluid mechanics can be divided into fluid statics (study of fluids at rest) and fluid dynamics (study of fluids in motion).

1.2.4 Deformation

The relative change in position or length of the fluid particles is known as deformation (strain).

1.2.5 Shear stress

A shear stress, denoted by τ (tau) is defined as a stress which is applied parallel or tangential to a face of a material, as opposed to a normal stress which is applied normally (perpendicularly).

1.2.6 Pressure

Pressure is defined as the magnitude of force per unit area and it can be written as

$$P = \frac{F}{A},\tag{1.1}$$

where P is pressure, F is the magnitude of normal force and A is the area.

1.2.7 Density

The density of a fluid is defined as its amount of mass per unit volume. It is denoted by the Greek symbol ρ. Mathematically, it can be written as

$$\rho = \frac{m}{V},\tag{1.2}$$

where m is the mass and V is the volume.

1.2.8 Viscosity

Viscosity of the fluid is defined as the property of the fluid that tends to resist the movement of one layer of the fluid over adjacent layer of the fluid. It is denoted by the symbol μ and is defined as

$$\mu = \frac{\text{shear stress}}{\text{rate of shear strain}}.\tag{1.3}$$

It is also termed as dynamic viscosity.

5

1.2.9 Kinematic viscosity

It is defined as the ratio of dynamic viscosity to fluid density and is denoted by ν. Mathematically, it is defined as

$$\nu = \frac{\mu}{\rho}. \tag{1.4}$$

1.2.10 Viscous dissipation

An important consequence of the existence of shear viscosity is a loss of energy when fluid is sheared. This frictional energy loss is referred to as viscous dissipation. The rate of dissipation of energy per unit mass of fluid by the shear viscosity is given by the viscous dissipation ϕ. The viscous dissipation rate at any point in the flow is given by

$$\phi = \frac{2\mu}{\rho} \left(\frac{du}{dy} \right)^2, \tag{1.5}$$

where du/dy is the rate of shear strain.

1.2.11 Shear thinning effect

Shear thinning is an effect where viscosity decreases with increasing rate of shear stress. Materials that execute shear thinning are called pseudoplastic. There are certain complex solutions such as lava, ketchup, whipped cream, blood, paint and nail polish which describe such effects.

1.2.12 Shear thickening effect

A shear thickening effect is one in which viscosity of a fluid increases with the rate of shear stress. Fluids which describe such effects are termed as dilatant. Mixture of cornstarch and water can easily be seen to perform this effect.

6

1.3   Classification of fluid

1.3.1   Ideal fluid

A non-existent, assumed fluid without either viscosity or compressibility is called an ideal or perfect fluid. It is the hypothetical form of fluids. However, the fluid with negligible viscosity may be considered as an ideal fluid.

1.3.2   Real fluid

Real fluids are those in which fluid friction has significant effects on the fluid motion. In other words, we can not neglect the viscosity effects on the motion. Real fluids are further classified into two classes on the basis of *Newton's law of viscosity*. According to this law "shear stress is directly proportional to the rate of deformation". For one dimensional flow, it can be written as

$$\tau_{yx} = \mu \frac{du}{dy}, \tag{1.6}$$

where τ_{yx} is the shear stress.

Newtonian fluid

A Newtonian fluid (named after *Isaac Newton*) is a fluid whose stress versus strain (deformation) rate curve is linear and passes through the origin, i.e., Newtonian fluid obeys *Newton's law of viscosity*. Water, gasoline and mercury are some examples of Newtonian fluids.

Non-Newtonian fluid

Fluids in which shear stress is not directly proportional to the deformation rate are known as non-Newtonian. A non-Newtonian fluid is a fluid whose flow properties are not described by a single constant value of viscosity, i.e., it does not satisfy *Newton's law of viscosity*. For non-Newtonian fluids

$$\tau_{yx} = k \left(\frac{du}{dy} \right)^n, \qquad n \neq 1 \tag{1.7}$$

or

$$\tau_{yx} = \eta \left(\frac{du}{dy} \right), \tag{1.8}$$

7

where

$$\eta = k \left(\frac{du}{dy} \right)^{n-1} \tag{1.9}$$

is the apparent viscosity. Examples of non-Newtonian fluids are tooth paste, ketchup, gel, shampoo, blood and soaps etc.

1.4 Types of flow

1.4.1 Steady flow

A flow for which the fluid properties (velocity, temperature etc.) remain independent of time is called steady flow. For such flow

$$\frac{\partial Q}{\partial t} = 0, \tag{1.10}$$

where Q is any quantity in the flow and t is the time.

1.4.2 Unsteady flow

A flow for which fluid velocity depends upon time is called unsteady flow, i.e.

$$\frac{\partial Q}{\partial t} \neq 0. \tag{1.11}$$

1.4.3 Laminar flow

Fluid flow in which the fluid travels smoothly or in regular paths. Laminar flow over a horizontal surface may be thought of as consisting of thin layers, all parallel to each other that slide over each other. Examples include the flow of oil through a thin tube and blood flow through capillaries.

1.4.4 Turbulent flow

Turbulent flow is a type of fluid flow in which the fluid undergoes irregular fluctuations or mixing. Common examples of turbulent flow are lava flow, atmosphere and ocean currents, the flow through pumps and turbines and the flow in boat wakes and around aircraft-wing tips.

1.4.5 Incompressible flow

A flow in which the volume and thus the density of the flowing fluid does not change during the flow. All the liquids are generally considered to have incompressible flow. Incompressible flow satisfies the equation

$$\nabla.\vec{V} = 0, \tag{1.12}$$

where $\vec{V}$ is the velocity field of the flow.

1.4.6 Compressible flow

A flow, in which the volume and thus density of the flowing fluid changes during the flow. All gases are, generally, considered to have compressible flows. For compressible flow

$$\nabla.\vec{V} \neq 0. \tag{1.13}$$

1.5 Force

Force is a vector quantity, used to demonstrate an impression which causes a free body to undergo a change in velocity or acceleration.

1.6 Types of forces

1.6.1 Surface force

Short-range force applying on a fluid element through physical contact between the element and its forcing body is called surface force.

1.6.2 Body force

Body force is long-range force that acts on a small fluid elements. Gravitational and electromagnetic forces are the common examples of body force. It is usually denoted by the symbol f.

9

1.7 Heat transfer

Heat transfer is a science that studies the energy transfer between two bodies due to temperature difference. There are three types or modes of heat transfer:

1. Conduction
2. Convection
3. Radiation

1.8 Fundamentals of heat transfer

1.8.1 Conduction

Conduction is the transfer of energy through matter from particle to particle. It is the transfer and distribution of heat energy from atom to atom within a substance. For example, a spoon in a cup of hot soup becomes warmer because the heat from the soup is conducted along the spoon. Conduction is most effective in solids but it can happen in fluids.

1.8.2 Convection

Convection is the transfer of heat by the actual movement of the warmed matter. Heat leaves the coffee cup as the currents of steam and air rise. Convection is the transfer of heat energy in a gas or liquid by movement of currents. (It can also happen is some solids, like sand).

1.8.3 Radiation

Electromagnetic waves that directly transport energy through space. Sunlight is a form of radiation that is radiated through space to our planet without the aid of fluids or solids.

1.8.4 Specific heat

Specific heat is the amount of heat or thermal energy required to raise the temperature of a unit quantity of a body by one unit. It is denoted by the symbol c_p.

1.8.5 Fourier's law of heat conduction

The Fourier's law states that the time rate of heat transfer through a material is proportional to the negative gradient in the temperature and to the area at right angles to that gradient through which the heat is flowing. Mathematically, it is given by

$$\frac{dQ}{dt} = -kA\frac{d\theta}{dx},$$ (1.14)

where Q is the amount of heat transferred and θ is the temperature.

1.8.6 Thermal conductivity

Thermal conductivity k is the property of a material that indicates its capability to conduct heat.

1.9 Some Basic laws

1.9.1 Law of conservation of mass

This law states that in any closed system, the mass is always invariant regardless of its changes in shape. It is the principle which describes that matter cannot be created or destroyed. In fluid mechanics, this law is named as equation of continuity. Mathematically, it is described as

$$\frac{\partial \rho}{\partial t} + \nabla \cdot (\rho \mathbf{V}) = 0.$$ (1.15)

For steady flow

$$\frac{\partial \rho}{\partial t} = 0,$$ (1.16)

and for steady incompressible flow

$$\rho(\nabla \cdot \mathbf{V}) = 0.$$ (1.17)

11

1.9.2 Law of conservation of momentum

The law of conservation of momentum states that when some bodies constituting an isolated system act upon one another, the total momentum of the system remains same. It is also recognized as the Navier-Stokes equations derived by *Claude-Louis Navier* and *George Gabriel Stoke*, used to describe the motion of the fluid. In an inertial frame of reference, the general form of the equations of fluid motion is

$$\rho\frac{D\mathbf{V}}{Dt} = \mathbf{\nabla} \cdot \mathbf{T} + \mathbf{f}, \tag{1.18}$$

where $\mathbf{T}$ is the Cauchy stress tensor which is different for different fluids.

1.9.3 Law of conservation of energy

The law of conservation of energy states that energy may neither be created nor destroyed. Therefore, the sum of all the energies in the system is a constant. The laws of conservation of energy which is also called the energy equation is described as

$$\rho c_p \frac{D\theta}{Dt} = \mathbf{T} \cdot \mathbf{L} - \mathbf{\nabla} \cdot \mathbf{q}, \tag{1.19}$$

in which

$$\mathbf{L} = \mathbf{\nabla}\mathbf{V}. \tag{1.20}$$

1.10 Boundary layer

The flow region adjacent to the wall in which the viscous effects are significant is called boundary layer.

1.10.1 Boundary layer thickness

The boundary layer thickness, signified by δ is simply the thickness of the viscous boundary layer region. Because the main effect of viscosity is to slower the fluid near a wall, the edge of the viscous region is found at the point where the fluid velocity is essentially equal to the free-stream velocity.

1.11 Homotopy

A homotopy between two functions f and g from a space X to a space Y is a continuous map H,

$$H : X \times [0,1] \longrightarrow Y, \qquad (1.21)$$

such that

$$H(x,o) = f(x) \qquad (1.22)$$

and

$$H(x,1) = g(x), \qquad (1.23)$$

where X denotes set pairing and $x \in X$. If we consider the second element in the set $X \times [0,1]$, then we can say that at time $t = 0$, the function H equals f and at $t = 1$, H becomes g. Two mathematical objects are said to be homotopic if one can be continuously deformed into the other. The concept of homotopy was first formulated by *Poincaré* around 1900 (*Collins* 2004). When two functions f and g are homotopic, we relate them as

$$f \simeq g. \qquad (1.24)$$

1.11.1 Homotopy analysis method (HAM)

Perturbation methods have been widely used by the engineers in obtaining results especially for non-linear problems. Such methods require small or large parameters so that approximate solution can be expressed in term of series. It is not necessary that all problems involve such small or large parameters. Therefore it seems important to have another analytic method which does not required the restriction on parameters. Keeping this fact in view, Liao has developed homotopy analysis method (HAM) which is independent upon small parameters assumption. The basic idea of HAM is described as follows.

Consider a non-linear equation governed by

$$N[u(x,t)] = 0, \qquad (1.25)$$

where N is non-linear operator, x and t denote the independent variables and u is an unknown

function. For simplicity, we ignore all boundary and initial conditions, which can be treated in the similar way. By means of HAM, we first construct the so-called zeroth-order deformation equation as

$$(1 - q)L[\Phi(x, t; q) - u_0(x, t)] = q\hbar H(x, t)N[\Phi(x, t; q)] \qquad (1.26)$$

where $q \in [0, 1]$ is the embedding parameters, $\hbar \neq 0$ is an auxiliary parameter, L is an auxiliary linear operator , $\Phi(x, t; q)$ is unknown function, $u_0(x, t)$ is an initial guess and $H(x, t)$ denote a non-zero auxiliary function. It is obvious that for embedding parameter $q = 0$ and $q = 1$, equation (1.27) becomes

$$\Phi(x, t; 0) = u_0(x, t), \qquad N[\Phi(x, t; 1)] = 0,$$

respectively. Thus as q increases from 0 to 1, the solution $\Phi(x, t; q)$ varies from the initial guess $u_0(x, t)$ to the solution $u(x, t)$. Expanding $\Phi(x, t; q)$ in Taylor series with respect to q, one has

$$\Phi(x, t; q) = u_0(x, t) + \sum_{m=1}^{+\infty} u_m(x, t)q^m, \qquad (1.27)$$

where

$$u_m(x, t) = \frac{1}{m!} \frac{\partial^m \Phi(x, t; q)}{\partial q^m} \Big|_{q=0}, \qquad (1.28)$$

The convergence of the series (1.28) depends upon the auxiliary parameter $\hbar$. It is convergent at $q = 1$, one has

$$u(x, t) = u_0(x, t) + \sum_{m=1}^{+\infty} u_m(x, t), \qquad (1.29)$$

which must be one of the solutions of the original non-linear equation, as proven by Liao [18]. Define a vector

$$\overrightarrow{u}_n = \{u_0(x, t), u_1(x, t), \cdots, u_n(x, t)\}.$$

Differentiating the *zeroth − order* deformation equation (1.27) *m − times* with respect to q

14

and dividing by the $m!$ and finally setting $q = 0$, we get the following $mth - order$ deformation equation

$$L[u_m(x,t) - \chi_m u_0(x,t)] = hH(x,t)R_m[\vec{u}_{m-1}], \qquad (1.30)$$

where

$$R_m[\vec{u}_{m-1}] = \frac{1}{(m-1)!}\frac{\partial^{m-1}N[\Phi(x,t;q)]}{\partial q^{m-1}}\Big|_{q=0} \qquad (1.31)$$

and

$$\chi_m = \begin{cases} 0, k \leq 1 \\ 1, k > 1 \end{cases}. \qquad (1.32)$$

It should be emphasized that $u_m(x,t)$ for $m \geq 1$ is governed by the linear equation (1.31) with linear boundary conditions that come from the original problem, which can be solved by symbolic computation software such as Maple or Mathematica.

1.11.2   Homotopy-Padé approximation

A Padé approximation of a given power series is a rational function of numerator of *degree* m and denominator of *degree* n whose power series agrees with the given one upto *degrees* $m + n$ inclusively. The Padé approximation can be though of as a generalization of a Taylor Polynomial. A Padé approximation often yields better approximation of the function that truncating its Taylor series, and it may still work where the Taylor series does not converge. In many cases traditional Padé technique can greatly increase the convergence region and rate of approximations. For a given series

$$\sum_{n=0}^{\infty} a_n r^n. \qquad (1.33)$$

The corresponding $[m,n]$ Padé approximation is

$$\frac{\sum\limits_{k=0}^{m} b_{m,k} r^k}{\sum\limits_{k=0}^{m} c_{m,k} r^k} \tag{1.34}$$

in which $b_{m,k}$ and $c_{m,k}$ are determined by the coefficients a_i $(i = 0, 1, 2, 3, \cdots, m + n)$. The so-called homotopy-Padé approximation was proposed by combining the Padé approximation and homotopy analysis method. For convergence of series Eq.(1.28) at $q = 1$, we first employ the traditional $[m, n]$ Padé technique about the embedding parameter q to obtain $[m, n]$ Padé approximant

$$\frac{\sum\limits_{k=0}^{m} B_{m,k}(r) q^k}{\sum\limits_{k=0}^{m} C_{m,k}(r) q^k}, \tag{1.35}$$

where the coefficients $B_{m,k}(r)$ and $C_{m,k}(r)$ are determined by the first several approximations $u_0(r), u_1(r), u_2(r) \cdots, u_{m+n}(r)$. On setting $q = 1$ equation (1.36) becomes

$$\frac{\sum\limits_{k=0}^{m} B_{m,k}(r)}{\sum\limits_{k=0}^{m} C_{m,k}(r)}. \tag{1.36}$$

In general the $[m, m]$ homotopy-Padé expression can be expressed as.

$$\frac{\sum\limits_{k=0}^{m^2+m+1} B_1^{m,k}(r)}{\sum\limits_{k=0}^{m^2+m+1} C_1^{m,k}(r)}. \tag{1.37}$$

In above equation $B_1^{m,k}(r)$ and $C_1^{m,k}(r)$ are coefficients. It is very interesting that these coefficients are independent of the auxiliary parameter $\hbar$. Comparing equations (1.35) and (1.38), we find that in accuracy the $[m, m]$ homotopy-Padé approximation is equivalent to the traditional $[m^2 + m + 1, m^2 + m + 1]$ Padé approximant. Similarly, the so-called homotopy-Padé approximation can be applied to accelerate the convergence of the related series.

16

Chapter 2

A new branch of solutions of boundary-layer flows over an impermeable stretched plate

2.1 Introduction

The boundary layer flows over the stretched impermeable wall were investigated by different authors so far by using different homotopy analysis method and numerical schemes etc. Two branches of the solutions are found. The first one agrees well with the numerical results given by Bank [3]. However, the second branch can further be divided into two parts in which one is mathematically equivalent to a branch of solutions of Cheng and Minkowycz's equation reported by the Ingham et al [17]. The other one is new and has never been reported other than Liao [15]. In this chapter we revise the study of Liao [15]. It is also analyzed that different from the first branch of solutions the second branch of solution shows reversed velocity flows. It is further observed that the difference of skin frictions of the two branches of solutions is rather small, even when the corresponding profiles of velocity are clearly distinct.

2.2 Problem Formulation

Consider the boundary-layer viscous flow over a stretched impermeable plate [2, 3] governed by

$$u\frac{\partial u}{\partial x} + v\frac{\partial u}{\partial y} = \nu\frac{\partial^2 u}{\partial y^2}, \tag{2.1}$$

$$\frac{\partial u}{\partial x} + \frac{\partial v}{\partial y} = 0, \tag{2.2}$$

subject to the boundary conditions

$$\left.\begin{array}{cccc} u = a(x+b)^\lambda, & v = 0 & at & y = 0, \\ u \longrightarrow 0 & as & y \longrightarrow +\infty \end{array}\right\}. \tag{2.3}$$

Where (x, y) denotes the Cartesian coordinates along the plate and normal to it, u and v are the velocity components of fluid in the x and y directions, ν is kinematic viscosity, a, b and λ are parameters related to the surface stretching speed. Let Ψ denote the stream function. Using the transformation

$$\left.\begin{array}{c} \Psi = a\sqrt{\dfrac{\nu}{a(1+\lambda)}}(x+b)^{\frac{\lambda+1}{2}} F(\xi), \\ \xi = \sqrt{\dfrac{a(1+\lambda)}{\nu}}(x+b)^{\frac{\lambda-1}{2}} y \end{array}\right\}, \tag{2.4}$$

where $a \neq 0$ and $a(1+\lambda) > 0$, the above equations become

$$F'''(\xi) + \frac{1}{2}F(\xi)F''(\xi) - \beta F'^2(\xi) = 0, \tag{2.5}$$

subject to the boundary conditions

$$F(0) = 0, \qquad F'(0) = 1, \qquad F'(+\infty) = 0, \tag{2.6}$$

where

$$\beta = \frac{\lambda}{1+\lambda}. \tag{2.7}$$

Since $a(1+\lambda) > 0$, we have a>0 when $\lambda > -1$, corresponding to $-1 < \beta \leqslant 1$; and a<0 when $\lambda < -1$, corresponding to $\beta > 1$. When, $a < 0$ and $-1 < \beta \leqslant 1$, the stretching velocity

18

of the surface is positive. However, when $a < 0$ and $\beta > 1$, the stretching velocity becomes negative, corresponding to the so called backward boundary layer that has physical meanings as mentioned by Goldstein [13].

From Eq.(2.4), we deduce the velocity of the fluid

$$u(x,y) = a(x+b)^{\lambda} F'(\xi), \tag{2.8}$$

$$v(x,y) = \frac{-1}{2}\sqrt{a(1+\lambda)\nu}(x+b)^{\frac{\lambda-1}{2}}[F(\xi) + (2\beta-1)\xi F'(\xi)]. \tag{2.9}$$

The velocity of the fluid at $\xi \longrightarrow +\infty$ is

$$v(x,+\infty) = \frac{-1}{2}\sqrt{a(1+\lambda)\nu}(x+b)^{\frac{\lambda-1}{2}}F(+\infty), \tag{2.10}$$

and the skin friction on the stretched surface becomes

$$\tau_w = \rho\nu\frac{\partial u}{\partial y}\mid_{y=0} = a\rho\sqrt{a(1+\lambda)\nu}(x+b)^{\frac{3\lambda-1}{2}}F''(0). \tag{2.11}$$

Banks [3] gave a branch of solution for $-1 < \beta < +\infty$ by using numerical method, also satisfied the property $F'(\xi) > 0$ for $0 < \xi < +\infty$. As pointed by Chaudhary et al. [10], Magyari and Keller [12], and reported by Liao and Pop [15], the considered problem is mathematically equivalent to the steady free convection flow over a vertical semi-infinite plate that is embedded in a fluid saturated porous medium, described by famous Cheng and Minkowycz's equation [16], if and only if $\lambda > -1/2$ corresponding to $-1 < \beta \leq 1$. It is easy to verify that the first branch of solutions reported by Ingham and Brown [17] is indeed mathematically equivalent to those given by Banks [3] in a finite region $-1 < \beta \leq 1$. Note that the two problems are not completely equivalent even mathematically. Ingham and Brown [17] proved that there is no solution corresponding to the forward boundary layer flows for the Cheng and Minkowycz's equation when $\lambda \leq -1$, corresponding to $\beta > 1$. However, Banks [3] found numerical results even for $\beta = 200$. It is interesting that Ingham and Brown [17] reported a second branch of solution for $1 \leq \lambda < +\infty$, corresponding to $1/2 \leq \beta < 1$. According to the above-mentioned equivalence between the two problems, Eqs.(2.5) and (2.6) should have multiple solutions at

19

least in the region $-1/2 < \beta \leq 1$. But Banks [3] did not mention such kind of solutions. Employing the homotopy analysis method [18-20], a new analytic technique for non-linear problems, Liao and Pop [15] successfully found the first branch of solutions which agree well with the Banks numerical results, but equally fail to find the second ones.

In this chapter, a new branch of solutions is reproduced for $1/2 < \beta < +\infty$ by means of the homotopy analysis method [18, 19], which has been successfully applied to solve many non-linear problems. In a finite region $1/2 \leq \beta \leq 1$, this kind of branch of solutions is mathematically equivalent to the second branch of solutions of the Cheng and Minkowycz's equation given by Ingham and Brown [17].

2.3   Mathematical Formulations

2.3.1   Asymptotic Property

According to the boundary condition $F'(+\infty) = 0$, it is straightforward to define

$$\delta = F(+\infty). \tag{2.12}$$

It is well-known that most boundary-layer flows have exponential property at unity. Thus, it is natural to express $F(\xi)$ as

$$F(\xi) = \delta + \sum_{j=1}^{+\infty} A_j \exp(-j\mu\xi), \tag{2.13}$$

where $\mu > 0$ is the spatial-scale parameter and A_j is a coefficient. When $\xi \longrightarrow +\infty$, the dominant term of the above expression is

$$F(\xi) \approx \delta + A_1 \exp(-\mu\xi),$$

Substituting it into Eq.(2.5), we have

$$\frac{-A_1\mu^2}{2}(2\mu - \delta)\exp(-\mu\xi) - \frac{-A_1^2\mu^2}{2}\exp(-2\mu\xi) + \cdots = 0, \ \xi \longrightarrow +\infty.$$

To enforce the dominant term of the above equation is zero, we set

$$\mu = \delta/2, \tag{2.14}$$

which enforces

$$\delta > 0. \tag{2.15}$$

Thus, under the transformation

$$F(\xi) = \delta[1 - w(\eta)], \qquad \eta = (\frac{\delta}{2})\xi. \tag{2.16}$$

Eq.(2.5) becomes

$$w'''(\eta) + [1 - w(\eta)]w''(\eta) + 2\beta w'^2(\eta) = 0, \qquad \eta \in [0, +\infty), \tag{2.17}$$

subject to the boundary conditions

$$w(0) = 1, \qquad w'(0) + 2\gamma = 0, \qquad w'(+\infty) = 0, \qquad w(+\infty) = 0, \tag{2.18}$$

where

$$\gamma = \frac{1}{\delta^2} \tag{2.19}$$

depends on β. Note that γ does not appear in Eq.(2.17). If β is given, then the unknown γ must be determined. Similarly, if γ is given, we should regard β as an unknown parameter.

In the frame of the homotopy analysis method [18, 19], Eqs.(2.17) and (2.18) can be solved by three different approaches, as described below.

2.3.2 First approach for given β

Zeroth-order deformation equation

$w(\eta)$ can be expressed by the base functions

$$\{exp(-n\eta) \mid n \geq 1\}$$

21

in the form

$$w(\eta) = \sum_{j=1}^{+\infty} A_j \exp(-j\eta). \tag{2.20}$$

For given β, γ is unknown. Let γ_0 denote the initial approximation of γ where γ_0 is unknown. Under the Rule of Solution expression (2.20) and using the boundary conditions (2.18), it is straightforward to choose

$$w_0(\eta) = 2(1 - \gamma_0) \exp(-\eta) + (2\gamma_0 - 1) \exp(-2\eta) \tag{2.21}$$

as the initial approximation of $w(\eta)$. Under the Rule of Solution Expression(2.20) and with the aid of governing equation (2.17), the auxiliary linear operator is defined as

$$\mathcal{L}[\Phi(\eta; q)] = \frac{\partial^3 \Phi(\eta; q)}{\partial \eta^3} + 2\frac{\partial^2 \Phi(\eta; q)}{\partial \eta^2} - \frac{\partial \Phi(\eta; q)}{\partial \eta} - 2\Phi(\eta; q). \tag{2.22}$$

It possesses the property

$$\mathcal{L}[C_1 e^{-\eta} + C_2 e^{-2\eta} + C_3 e^{2\eta}] = 0, \tag{2.23}$$

for any constants C_1, C_2 and C_3. Furthermore, Eq.(2.17) suggests to define the non-linear operator as

$$\mathcal{N}[\Phi(\eta; q)] = \frac{\partial^3 \Phi(\eta; q)}{\partial \eta^3} + [1 - \Phi(\eta; q)]\frac{\partial^2 \Phi(\eta; q)}{\partial \eta^2} + 2\beta[\frac{\partial \Phi(\eta; q)}{\partial \eta}]^2. \tag{2.24}$$

Let $q \in [0, 1]$ denote an embending parameter, $\hbar \neq 0$ an auxiliary parameter, and $H(\eta) \neq 0$ an auxiliary function. Using above definitions, we construct the zeroth-order deformation equation

$$(1 - q)\mathcal{L}[\Phi(\eta; q) - w_0(\eta)] = q\hbar H(\eta)N[\Phi(\eta; q)], \tag{2.25}$$

subject to the boundary conditions

$$\Phi(0; q) = 1, \qquad 2\Gamma(q) + \frac{\partial \Phi(\eta; q)}{\partial \eta} \mid_{\eta=0} = 0, \qquad \lim_{\eta \longrightarrow +\infty} \frac{\partial \Phi(\eta; q)}{\partial \eta} = 0. \tag{2.26}$$

22

When $q = 0$ and $q = 1$, we have from the zeroth-order deformation equations (2.25) and (2.26) that

$$\Phi(\eta; 0) = w_0(\eta), \qquad \Gamma(0) = \gamma_0, \qquad (2.27)$$

and

$$\Phi(\eta; 1) = w(\eta), \qquad \Gamma(1) = \gamma, \qquad (2.28)$$

respectively. Defining

$$w_n(\eta) = \frac{1}{n!} \frac{\partial^n \Phi(\eta; q)}{\partial q^n} \Big|_{q=0}, \qquad \gamma_n = \frac{1}{n!} \frac{\partial^n \Gamma(q)}{\partial q^n} \Big|_{q=0}$$

and expending $\Phi(\eta; q)$ and $\Gamma(q)$ in Taylor series with respect to the embending parameter q, we have

$$\Phi(\eta; q) = \Phi(\eta; 0) + \sum_{n=1}^{+\infty} w_n(\eta) q^n, \qquad (2.29)$$

$$\Gamma(q) = \Gamma(0) + \sum_{n=1}^{+\infty} \gamma_n q^n. \qquad (2.30)$$

Assuming that $\hbar$ and $H(\eta)$ are properly chosen so that the above series converge at $q = 1$, we have from Eqs.(2.27) and (2.28) that

$$w(\eta) = w_0(\eta) + \sum_{n=1}^{+\infty} w_n(\eta), \qquad (2.31)$$

$$\gamma = \gamma_0 + \sum_{n=1}^{+\infty} \gamma_n. \qquad (2.32)$$

Higher-order deformation equation

For the sake of simplicity, define the vector

$$\vec{w}_m(\eta) = \{w_0(\eta), w_1(\eta), w_2(\eta), \cdots w_m(\eta)\},$$

23

differentiating the zeroth-order deformation Eqs.(2.25) and (2.26) n times with respect to the embending parameter q, then setting $q = 0$, and finally dividing by $n!$, we have the nth-order deformation equation

$$\mathcal{L}[w_n(\eta) - \chi_n w_{n-1}(\eta)] = \hbar H(\eta) R_n[\overrightarrow{w}_{n-1}(\eta), \gamma_{n-1}], \tag{2.33}$$

subject to the boundary conditions

$$w_n(0) = 0, \qquad w_n'(0) + 2\gamma_n = 0, \qquad w_n'(\infty) = 0, \tag{2.34}$$

under the definitions

$$R_n[\overrightarrow{w}_{n-1}(\eta), \gamma_{n-1}] = w'''(\eta) + w''(\eta) + \sum_{i=0}^{n-1} [2\beta w_i'(\eta) w_{n-1-i}'(\eta) - w_i''(\eta) w_{n-1-i}(\eta)]. \tag{2.35}$$

and

$$\chi_k = \begin{cases} 0, & k \leq 1 \\ 1, & k > 1 \end{cases}. \tag{2.36}$$

Due to the boundary conditions (2.34), $w_k(\eta)$ contains the unknown γ_k for $k = 0, 1, 2, 3, \cdots$. Thus, the term $R_n[\overrightarrow{w}_{n-1}(\eta), \gamma_{n-1}]$ contains the unknown γ_{n-1}. Note that both $w_n(\eta)$ and γ_{n-1} are unknown, but we have only Eqs.(2.33) and (2.34) for $w_n(\eta)$. Thus, the problem is not closed and an additional algebraic equation is needed to determine γ_{n-1}.

Substituting Eq.(2.21) into Eq.(2.35), we have

$$R_1[\overrightarrow{w}_0(\eta), \gamma_0] = \sum_{j=2}^{4} B_{1,j}(\gamma_0) \exp(-j\eta),$$

where $B_{1,j}(\gamma_0)$ is a coefficient dependent upon γ_0. According to the Rule of Solution Expression (2.20), the auxiliary function $H(\eta)$ must have the form

$$H(\eta) = \exp(k\eta)$$

where k is an integer. So, we have

24

$$H(\eta)R_1[\vec{w}_0(\eta), \gamma_0] = \sum_{i=2}^{4} B_{1,i}(\gamma_0) \exp[-(i-k)\eta], \qquad (2.37)$$

when $k \geq 1$, the term $\exp(-\eta)$ appears on right hand side of Eq.(2.33). Thus according to Eq.(2.23), the corresponding solution $w_1(\eta)$ contains

$$\eta \exp(-\eta),$$

which however, disobeys the Rule of Solution Expression Eq.(2.20). When $k \leq 1$, the solution of Eq.(2.33) does not contain the term $\exp(-3\eta)$, and this disobeys the Rule of Coefficient Ergodicity, i.e. all coefficients in the solution expression Eq.(2.20) can be modified to ensure the completeness of the set of the base functions, as mentioned by Liao [18,p.21]. When $k = -1$, there does not exist an algebraic equation to determine γ_0 and therefore the problem is not closed. This however disobeys the Rule of Solution Existence described by Liao [18,p.21]. When $k = 0$, i.e.

$$H(\eta) = 1, \qquad (2.38)$$

we can set

$$B_{1,2}(\gamma_0) = 0, \qquad (2.39)$$

which provides us with an algebraic equation to determine the unknown γ_0. And in this way, Rule of Solution Expression, the Rule of Coefficient Ergodicity, and the Rule of Solution of Existence, are satisfied. Using Eqs.(2.21) and (2.37) and imposing henceforth $k = 0$ in the Eq.(2.37), we have the algebraic equation

$$(2\beta - 1)\gamma_0^2 - 4\beta\gamma_0 + 2\beta = 0, \qquad (2.40)$$

which has two different positive solutions

$$\gamma_0 = \frac{\sqrt{2\beta}}{\sqrt{2\beta} + 1}, \qquad \beta \geq 0, \qquad (2.41)$$

25

and

$$\gamma_0 = \frac{\sqrt{2\beta}}{\sqrt{2\beta - 1}}, \qquad\qquad \beta > 1/2. \qquad\qquad (2.42)$$

Where the range of β is determined by the definition Eq.(2.19). Each of the above expression corresponds to a branch of solution. It is found that, when $H(\eta) = 1$, we always have

$$R_n[\overrightarrow{w}_{n-1}(\eta), \gamma_{n-1}] = \sum_{j=2}^{2n+2} B_{n,j}(\gamma_{n-1}) \exp[-j\eta]. \qquad\qquad (2.43)$$

Thus in general, we can always obtain γ_{n-1} by solving the algebraic equation

$$B_{n,j}(\gamma_{n-1}) = 0. \qquad\qquad (2.44)$$

It is found that the above algebraic equation is always linear when $(n \geq 2)$, and the solution $w_n(\eta)$ obeys the Rule of Solution Expression Eq.(2.20). In this way, it is convenient to solve the linear higher-order deformation Eqs.(2.33) and (2.34) by means of a symbolic software such as Mathematica.

Multiple solutions

For a given β, the two different values of γ_0, given by Eqs.(2.41) and (2.42), correspond to the two different values of γ and the two different solutions of $w(\eta)$, respectively. For example, let us consider the case of $\beta = 1$. For each γ_0, we obtain

$$w_1(\eta), \gamma_1, w_2(\eta), \gamma_2 \cdots,$$

successively. Obviously, it is important to ensure that the series Eq.(2.31) and Eq.(2.32) are convergent due to auxiliary parameter $\hbar$, which can control the convergence of these series.

Note that γ is a function of $\hbar$. The so-called $\hbar$−curves of γ at the 10th-order of approximation are as shown in Fig. 2.1. Obviously, the series of γ converges when $\hbar = -1/2$ for the first branch of solutions, or when $\hbar = -3/4$ for the second branch. This is indeed true, as shown in Tables 1 and 2. Besides, much more accurate results can obtained by means of the so-called homotopy-

Padé technique [18, 20], as shown in Tables 3 and 4. The corresponding series of $w(\eta)$ also converges to the numerical results given by Runge-Kutta's method using the analytic results of $F''(0)$, as shown in Fig. 2.2.

Thus, when $\beta = 1$, the first approach gives two different solutions, corresponding to

$$F(+\infty) = 1.2807737812 \qquad F''(0) = -0.9063755237$$

and

$$F(+\infty) = 0.4336537219 \qquad F''(0) = -0.9133389388$$

respectively. The first branch of solution agrees well with Bank's numerical results [3]. As shown in Fig. 2.2, the second branch of solution shows in some region reversed velocity flows. The second one was not reported for the stretched impermeable wall. Note that, although there exists obvious differences between $F(+\infty)$ of two solutions, the difference between $F''(0)$ is small. This might be the reason why the second branch of solution was not found by the shooting method.

As mentioned before, when $\beta = 1$, the above mentioned second branch should be mathematically equivalent to the corresponding second branch of solutions of the Cheng and Minkowycz's equation at $\lambda \longrightarrow +\infty$. We compare the two solutions and find that this is indeed true. The series verifies the validity of prescribed approach. And this approach is valid for other values of β, as shown later. So, different from Banks [3] and Liao and Pop [15], it is successfully reproduced the two branches of solutions for the boundary-layer flows over a stretched impermeable plate.

In general, for given $\beta, (\beta > 0)$. We can find the first branch of solution $(0 \le \beta < +\infty)$ by means of Eq.(2.41) and the second one $(1/2 < \beta < +\infty)$ by Eq.(2.42). In each case, the convergent result can be obtained by choosing a proper $\hbar$ according to the corresponding $\hbar-$curves of γ. Besides, the homotopy-Padé technique can be applied to accelerate the convergence of the solution series, when necessary. The values of $F(+\infty)$ and $F''(0)$ of two branches of solutions are listed in Tables 5 and 6. It is found that, different from the first branch of solutions, the second branch of solutions shows the reversed velocity flows in some regions that become

larger and larger as β tends to 1/2, as shown in Fig. 2.3. The second branch of solutions for $1/2 < \beta \leq 1$ is mathematically equivalent to the Cheng and Minkowycz's equation. However, it should be emphasized that the second branch of solutions for $1 < \beta < +\infty$ has never been reported, to the best of our knowledge.
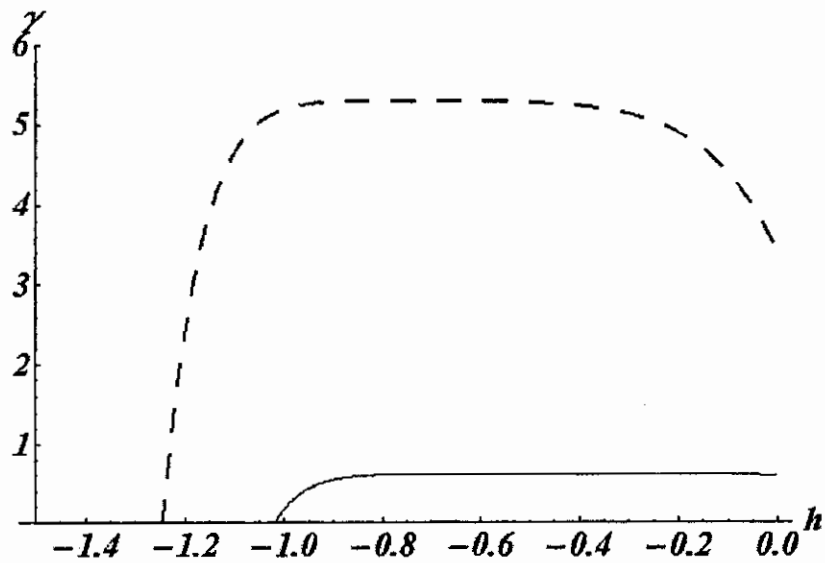

Fig. 2.1: $\hbar$-curves of γ at the 10*th*-order of approximations when $\beta = 1$: (solid line) for the first branch of solutions when $\gamma_0 = 2 - \sqrt{2}$ and (dashed line) for second branch of solution when $\gamma_0 = 2 + \sqrt{2}$.

Table 1:

Approximation of γ, $F(+\infty)$, and $F''(0)$ of the first branch of solutions when $\beta = 1, \gamma_0 = 2 - \sqrt{2}$ and $\hbar = -1/2$.

Order of Approximations	γ	$F(+\infty)$	$F''(0)$
5	0.60957	1.28083	-0.90621
10	0.60961	1.28077	-0.90638
20	0.60961	1.28077	-0.90638
30	0.60961	1.28077	-0.90638
40	0.60961	1.28077	-0.90638

Table 2:

Approximation of γ, $F(+\infty)$, and $F''(0)$ of the second branch of solutions when $\beta = 1, \gamma_0 = 2 + \sqrt{2}$ and $\hbar = -3/4$.

Order of Approximations	γ	$F(+\infty)$	$F''(0)$
10	5.31532	0.43375	-0.91243
20	5.31758	0.43365	-0.91334
30	5.31758	0.43365	-0.91334
40	5.31758	0.43365	-0.91334

Table 3:

The $[m, m]$ homotopy-Padé approximation of γ, $F(+\infty)$, and $F''(0)$ of the first branch of solutions when $\beta = 1, \gamma_0 = 2 - \sqrt{2}$.

$[m, m]$	γ	$F(+\infty)$	$F''(0)$
[5,5]	0.6096142954	1.2807737816	-0.9063755218
[10,10]	0.6096142958	1.2807737812	-0.9063755237
[15,15]	0.6096142958	1.2807737812	-0.9063755237
[20,20]	0.6096142958	1.2807737812	-0.9063755237

Table 4:

The $[m, m]$ homotopy-Padé approximation of γ, $F(+\infty)$, and $F''(0)$ of the second branch of solutions when $\beta = 1, \gamma_0 = 2 + \sqrt{2}$.

$[m, m]$	γ	$F(+\infty)$	$F''(0)$
[5,5]	5.3174870195	0.4336574191	-0.9133447576
[10,10]	5.3175776654	0.4336537229	-0.9133389444
[15,15]	5.3175776896	0.4336537219	-0.9133389388
[20,20]	5.3175776896	0.4336537219	-0.9133389388

Table 5:

$F(+\infty)$, and $F''(0)$ of the first branch of solutions when $\beta > 0$.

| β	$\hbar$	$F(+\infty)$	$F''(0)$
0.1	-1	1.5671987677	-0.5044714296
0.2	-1	1.5233211707	-0.5604081070
0.3	-1	1.4836193076	-0.6124206246
0.4	-1	1.4474244267	-0.6611548740
0.5	-1	1.4142135624	-0.7071067812
0.6	-1	1.3835703539	-0.7506652338
0.7	-1	1.3551581436	-0.7921407683
0.8	-1	1.3287010210	-0.8317853005
0.9	-1	1.3039701608	-0.8698060404
1	-1	1.2807737812	-0.9063755237
2	-1/2	1.1065468058	-1.2160186992
5	-1/3	0.8466059564	-1.8632196025
10	-1/5	0.6583880016	-2.6081483726
20	-1/7	0.4958786514	-3.6698608598
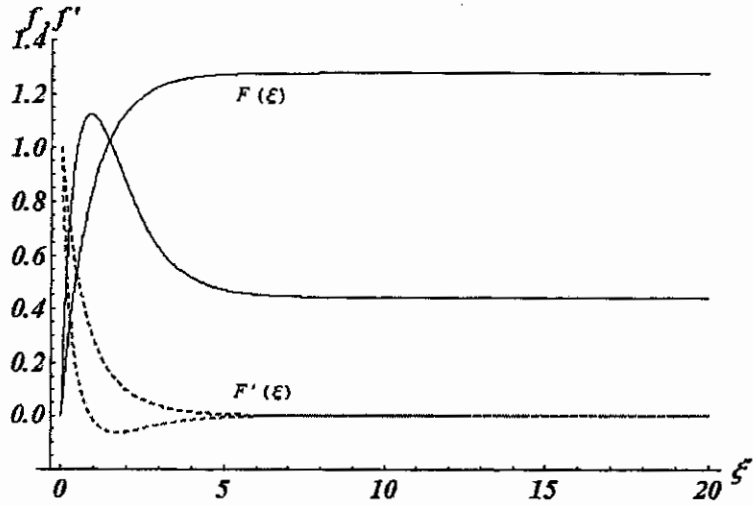
Fig 2.2: $F(\xi)$ and $F'(\xi)$ of the two branches of solutions when $\beta = 1$:(dashed line) $F(\xi)$ of the first branch of solution; (solid line) $F'(\xi)$ of the first branch of solutions; (dashed line) $F(\xi)$ for the second branch of solution; (dashed) $F'(\xi)$ of the second branch of solutions.
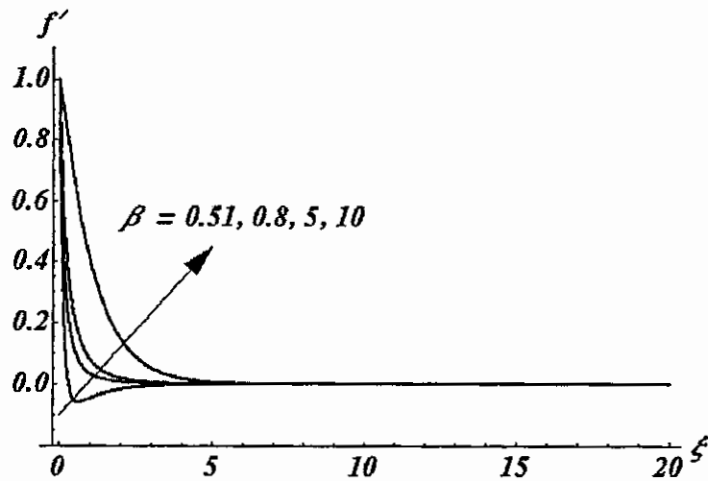

Fig 2.3: The second branch of the analytic solutions of the boundary-layer flows over a stretched wall.

31

Table 6:

$F(+\infty)$, and $F''(0)$ of the second branch of solutions when $1/2 < \beta < +\infty$.

β	$\hbar$	$F(+\infty)$	$F''(0)$
0.505	-1/40	0.1203123736	-0.71680431
0.51	-1/20	0.1350947640	-0.7194636996
0.53	-1/10	0.1708129121	-0.7290554847
0.55	-1/4	0.1956425368	-0.7381289899
0.6	-1/2	0.2423611636	-0.7598846445
0.8	-1/2	0.3597660152	-0.8401331462
1	-1/2	0.4336537219	-0.9133389388
1.5	-1/2	0.5402172761	-1.0760357869
2	-1/2	0.5934991205	-1.2185531166
3	-1/2	0.6351815454	-1.4644223721
4	-1/3	0.6416251516	-1.6756327445
5	-1/3	0.6347755047	-1.8634603629
10	-1/4	0.5646581867	-2.6081685246
20	-1/8	0.4579147612	-3.6698616153

In summary, by means of the above approach, we not only find the first branch of the solutions obtained by Banks [3], but also the second branch for $1/2 < \beta < +\infty$. Although the second branch of solutions for $1/2 < \beta \leq 1$ is mathematically equivalent to the second branch of solutions found by Ingham and Brown [17] for the Cheng and Minkowycz's equation, the second branch of solutions for $1 < \beta < +\infty$ is new investigation by Liao [25].

2.3.3 Second approach for given β

By means of the above-mentioned approach we can find the first branch of solutions in the region $\beta > 0$. However, as reported by Banks [3], the first branch of solutions exist for $-1 < \beta < +\infty$. So, we should give an analytic approach valid for $-1 < \beta < 0$.

For this purpose, we construct the zeroth-order deformation equation

$$(1 - q)\mathcal{L}[\Phi(\eta; q) - w_0(\eta)] = q\hbar\hat{H}(\eta)\mathcal{N}[\Phi(\eta; q)] \tag{2.45}$$

subject to the boundary conditions

$$\Phi(0; q) = 1, \qquad\qquad \lim_{\eta \longrightarrow \infty} \frac{\partial \Phi(\eta; q)}{\partial \eta} = 0, \tag{2.46}$$

and

$$\frac{\partial \Phi(\eta; q)}{\partial \eta} \Big|_{\eta=0} + 2(1 - q)\gamma_0 + 2q\Gamma(q) = 0, \tag{2.47}$$

where

$$\mathcal{L}[\Phi(\eta; q)] = \frac{\partial^3 \Phi(\eta; q)}{\partial \eta^3} - \frac{\partial \Phi(\eta; q)}{\partial \eta}, \tag{2.48}$$

with the property

$$\mathcal{L}[C_1 e^{-\eta} + C_2 + C_3 e^{\eta}], \tag{2.49}$$

The initial approximation $w_0(\eta)$ and the nonlinear operator N are the same as Eq.(2.21) and Eq.(2.24), respectively. Similarly, the series Eqs.(2.31) and (2.32) hold, and $w_n(\eta)$ is now governed by the higher-order deformation equations

$$\mathcal{L}[w_n(\eta) - \chi_n w_{n-1}(\eta)] = \hbar\hat{H}(\eta)R_n[\overrightarrow{w}_{n-1}(\eta), \gamma_{n-1}], \tag{2.50}$$

subject to the boundary conditions

$$w_n(0) = 0, \qquad w_n(\infty) = 0, \qquad w_n'(\infty) = 0 \tag{2.51}$$

and

$$w_n'(0) - 2\gamma_0(1 - \chi_n) + 2\gamma_{n-1} = 0, \tag{2.52}$$

where $R_n[\overrightarrow{w}_{n-1}(\eta), \gamma_{n-1}]$ is defined by Eq.(2.35). Similarly, to obey the Rule of Solution

33

Expression Eq.(2.20), we should choose

$$\hat{H}(\eta) = 1. \tag{2.53}$$

Let $w_n^*(\eta)$ denote the special solution of high-order deformation Eq. (2.50), which obeys the Rule of Solution Expression Eq.(2.20). Then, using the property Eq.(2.49), we have the general solution

$$w_n(\eta) = w_n^*(\eta) + C_1 e^{-\eta} + C_2 + C_3 e^{\eta}.$$

From Eq.(2.51) it obvious that $C_2 = C_3 = 0$. Then, C_1 is determined by the boundary condition $w_n(0) = 0$. For $n = 1$, $w_1(\eta)$ contains the unknown initial approximation γ_0, which is determined by the boundary condition Eq.(2.52), i.e.

$$w_1'(0) = 0. \tag{2.54}$$

It is found that Eq.(2.52) has two different solutions

$$\gamma_0 = \frac{51 + 8\beta - \sqrt{5(429 - 16\beta - 64\beta^2)}}{4(3 + 4\beta)} \tag{2.55}$$

and

$$\gamma_0 = \frac{51 + 8\beta + \sqrt{5(429 - 16\beta - 64\beta^2)}}{4(3 + 4\beta)}. \tag{2.56}$$

For $n > 1$, we have from Eq.(2.52) that

$$\gamma_{n-1} = -\frac{w_n'(0)}{2}, \qquad n \geq 2. \tag{2.57}$$

In this way, γ_{n-1} is obtained and all boundary conditions are satisfied. Note that, different from the first approach, the solution $w_n(\eta)$ given by the second approach does not contain the the unknown γ_n.

34

Table 7:

$F(+\infty)$, and $F''(0)$ of the first branch of solutions when $-1 < \beta \leq 0$.

β	$\hbar$	$F(+\infty)$	$F''(0)$
-0.95	-1	3.7343486357	2.777454210
-0.90	-1	3.1198300898	1.5176890220
-0.8	-1	2.5922842960	0.7135604366
-0.7	-1	2.3170430417	0.3660958444
-0.6	-1	2.1346791652	0.1528510095
-0.5	-1	2	0
-0.4	-1	1.8941059198	-0.1194986175
-0.3	-1	1.8073695138	-0.2181647105
-0.2	-1	1.7342480756	-0.3026969209
-0.1	-1	1.6712706089	-0.3770531959
0	-1	1.6161254468	-0.4437483134

Note that, γ_0 given by Eq.(2.55) is valid for

$$-\frac{\sqrt{430}+1}{8} < \beta < \frac{\sqrt{430}-1}{8}. \tag{2.58}$$

Besides, is tends to $2/9$ as $\beta \longrightarrow -3/4$. So, Eq.(2.55) is valid for $-1 \leq \beta \leq 0$. Similarly, for given β, we choose a proper $\hbar$ by plotting the corresponding $\hbar$–curves of γ, and besides the homotopy-Padé technique can be used to accelerate the convergence of the solution series, when necessary. In this way, using the initial approximation γ_0 given by Eq.(2.55), we obtain the first branch of solution in the region $-1 \leq \beta \leq 0$ is obtained, as shown in Table 7. The convergent analytic results for $\beta \leq -1$ cannot be obtained. All these analytic solutions agree well with Banks' numerical results [3] without reversed velocity flow.

Therefore, by means of the above two approaches for given β we can find the whole first branch of solutions given by Banks' numerical methods [3] and besides the whole second branch of solutions that shows reversed velocity flows in some regions. The values of $F(+\infty)$ of the two branches of solutions are as shown in Fig. 2.4.

35

Note that the second branch of solutions $1 < \beta < \infty$ has never been reported, although the solutions for $1/2 < \beta \leq 1$ are mathematically equivalent to Ingham and Brown's numerical solutions [17] for the Cheng and Minkowycz's equation.
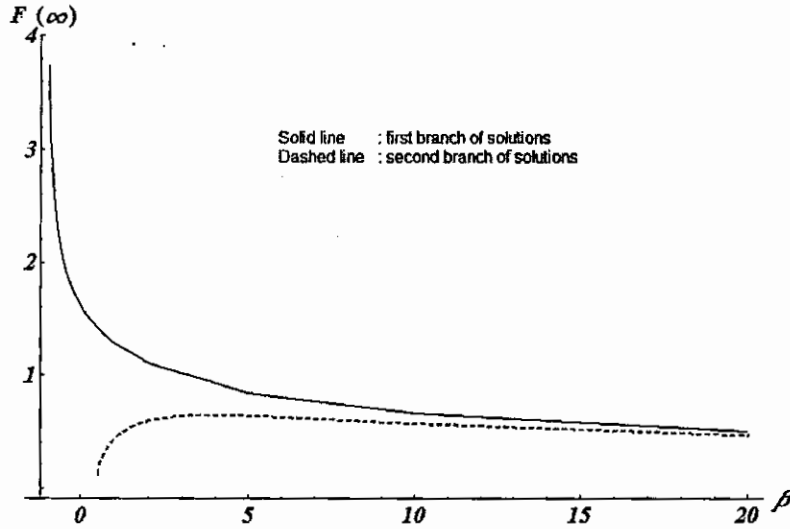

Fig. 2.4. Comparison of $F(+\infty)$ of the two branches of solutions of the boundary layer flows over a stretched wall: (solid line) first branch solutions; (dashed line) second branch solutions; results obtained by the approach for given entrainment velocity of the fluid.

2.3.4   Approach for given entertainment velocity

From Eq.(2.11), $F(+\infty)$ is related to the entertainment velocity of the fluid. Suppose that we would determine the movement of the stretched wall for a given entertainment velocity. This is an inverse problem and the corresponding approach is given below.

For a given $\gamma = 1/F^2(+\infty)$, we need to search for the corresponding value of β. Now, γ is known but β is unknown. So, we define a non-linear operator

$$\mathcal{N}[\Phi(\eta; q)] = \frac{\partial^3 \Phi(\eta; q)}{\partial \eta^3} + [1 - \Phi(\eta; q)]\frac{\partial^2 \Phi(\eta; q)}{\partial \eta^2} + 2\Lambda(q)[\frac{\partial \Phi(\eta; q)}{\partial \eta}]^2, \qquad (2.59)$$

where $\Lambda(q)$ corresponds to β. Using the initial guess

$$w_0(\eta) = 2(1 - \gamma)\exp(-\eta) + (2\gamma - 1)\exp(-2\eta) \qquad (2.60)$$

36

and the same auxiliary linear operator as in Eq.(2.22), we construct the zeroth-order deformation equation as follows

$$(1-q)\mathcal{L}[\Phi(\eta;q) - w_0(\eta)] = q\hbar H(\eta)\check{N}[\Phi(\eta;\Lambda(q))], \tag{2.61}$$

subject to the boundary conditions

$$\Phi(0;q) = 1, \qquad 2\gamma + \frac{\partial\Phi(\eta;q)}{\partial\eta}\,|_{\eta=0} = 0, \qquad \underset{\eta\to\infty}{Lim}\;\frac{\partial\Phi(\eta;q)}{\partial\eta} = 0 \tag{2.62}$$

where $\gamma = 1/F^2(+\infty)$ is known. Let β_0 denote the initial approximation of β. Write

$$\Lambda(q) = \beta_0 + \sum_{n=1}^{+\infty}\beta_n q^n \tag{2.63}$$

and

$$\overrightarrow{\beta}_m = \{\beta_0, \beta_1, \beta_2, \cdots \beta_m\},$$

where

$$\beta_n = \frac{1}{n!}\frac{\partial^n\Lambda(q)}{\partial q^n}\,|_{q=0}\;.$$

Similarly, from the zeroth-order deformation equations (2.61) and (2.62), we have the corresponding high-order deformation equation

$$\mathcal{L}[w_n(\eta) - \chi_n w_{n-1}(\eta)] = \hbar H(\eta)\check{R}_n[\overrightarrow{w}_{n-1}(\eta), \overrightarrow{\beta}_{n-1}]. \tag{2.64}$$

subject to the boundary conditions

$$w_n(0) = 0, \qquad w'_n(0) = 0, \qquad w'_n(\infty) = 0, \tag{2.65}$$

where

37

$$\check{R}_n[\vec{w}_{n-1}(\eta), \vec{\beta}_{n-1}] = w'''(\eta) + w''(\eta) - \sum_{k=0}^{n-1} w_k''(\eta) w_{n-1-k}(\eta) \left.\begin{array}{c} \\ \\ \\ \end{array}\right\} \cdot \qquad (2.66)$$
$$+2\sum_{k=0}^{n-1} \beta_{n-1-k} \sum_{i=0}^{k} w_i'(\eta) w_{k-i}'(\eta)$$

Similarly, we choose the auxiliary function

$$H(\eta) = 1.$$

Table 8:

The $[m,m]$ homotopy-Padé approximation of β and $F''(0)$ when $F(+\infty) = 2$.

$[m,m]$	γ	$F''(0)$
[5,5]	-0.4998755351	$4.6*10^{-4}$
[10,10]	-0.4999999350	$4.4*10^{-8}$
[15,15]	-0.4999999998	$1.3*10^{-11}$
[20,20]	-0.5000000000	$4.0*10^{-15}$

Let $B_{n,2}(\vec{\beta}_{n-1})$ denote the coefficient of $exp[-2\eta]$ of $\check{R}_n[\vec{w}_{n-1}(\eta), \vec{\beta}]$. Similarly, using the same auxiliary function as in Eq. (2.38) and enforcing

$$B_{n,2}(\vec{\beta}_{n-1}) = 0, \qquad (2.67)$$

We can obtain unknown $\vec{\beta}_{n-1}$. Thereafter, it is easy to get $w_n(\eta)$ of the high-order deformation Eq. (2.64) and Eq. (2.65)When $n = 1$, we have from Eq.(2.67) the initial approximation

$$\beta_0 = \frac{\gamma^2}{2(1-\gamma)^2} = \frac{1}{2(1-\delta^2)^2}, \qquad F(+\infty) = \delta = 1. \qquad (2.68)$$

Similarly, by means of plotting the $\hbar - curves$ of β and $F''(0)$, a proper value of $\hbar$ can be found to ensure that the solution series is converge, besides the homotopy-Padé technique may be applied to accelerate the convergence. For example, when $F(+\infty) = 2$, our analytic approximation converges to the exact solution

$$F(\eta) = 2\tanh(\eta/2), \qquad F''(0) = 0, \qquad \beta = 1/2,$$

as shown in Table 8. The values of $F''(0)$ and β for some given $F(+\infty)$ are listed in Table 9. All these results agree well with those given by the above-mentioned two approaches for the given β, as shown in Fig 4. This indicates the validity and flexibility of the homotopy analysis method. Besides, it also verifies the correctness of our second branch of solutions.

Table 9:

Approximations of β and $F''(0)$ for given $F(+\infty)$.

δ	$\hbar$	β	$F''(0)$
4	-3/4	-0.96177340	3.45489516
3	-3/4	-0.88397276	1.31559436
2.5	-3/4	-0.77171006	0.59275642
2	-3/4	-0.50000000	0.00000000
1.5	-3/4	0.25757399	-0.59078760
1.25	-1/10	1.14276743	-0.95635271
1.2	-1/50	1.40233554	-1.04147974
1.15	-1/50	1.70164153	-1.13211564
0.6	-3/5	2.09104978	-1.24285249
0.5	-3/4	1.26616358	-1.00298966
0.4	-2/5	0.89950383	-0.87728143
0.3	-3/10	0.68378517	-0.79457316
0.2	-1/10	0.55399162	-0.73990719
0.12	-3/50	0.50491551	-0.71675655
0.1	-1/25	0.50121417	-0.71436667
0.08	-3/100	0.50011008	-0.7129335

2.4 Analysis of the results and discussion

Using the above-mentioned three analytic approaches, we successfully reproduced two branches of solutions for the boundary-layer flows over a stretched impermeable wall. The first branch of solutions $(1 < \beta < +\infty)$ agrees well with Banks numerical results [3] given by shooting method, and do not show the reversed velocity flows. The second branch $(1/2 < b < +\infty)$ shows the reversed velocity flows in some regions that becomes larger and larger as β tends to 1/2. The second branch of solutions can be divided into two parts. One $(1/2 < \beta \leq 1)$ is mathematically equivalent to Ingham and Brown's second branch of numerical solutions of the Cheng and Minkowycz ' s equation [16], the other $(1 < \beta < +\infty)$ is reported by Liao[25]. The difference between the values of $F(+\infty)$ for the two branches of solutions is obvious near $\beta = 1/2$, but becomes smaller and smaller as β increases, as shown in Fig. 2.4. So, according to Eqs.(2.8) − (2.10), the velocity of the fluid and especially the entrainment velocity of the fluid of the two branches of solutions are different, especially near $\beta = 1/2$. However, the difference between the values of $F''(0)$ of the two branches of solutions is so small that it is even hard to distinguish them in Fig. 2.5. For example, the relative differences of $F''(0)$ when $\beta = 1, 5$ and 10 are 0.77%, 0.013%, and 0.00077%, respectively. According to Eq.(2.11), the local skin friction coefficient on the stretched wall is directly proportional to $F''(0)$. Thus, although the velocity profiles of the two branches of solutions of the boundary layer flows over a stretched wall might be obviously different, the skin frictions on the wall are nearly the same. So, from a practical point of view, we need not worry about the great increase of the skin friction on the wall when, owing to some reasons, the profile of the velocity and the entrainment velocity change from one of the two branches of solutions to the other.

It is well-known that, for some unsteady nonlinear problems, the tiny differences of initial conditions might lead to obviously different solutions. In this chapter, we show that the dual solutions of the boundary-layer flows over a stretched wall are sensitive to the boundary value $F''(0)$. Thus, mathematically speaking, for some nonlinear boundary value problems, the small difference of boundary conditions might also lead to obviously different solutions. This might be the reason why it is not easy to find the second branch of solutions by numerical methods.
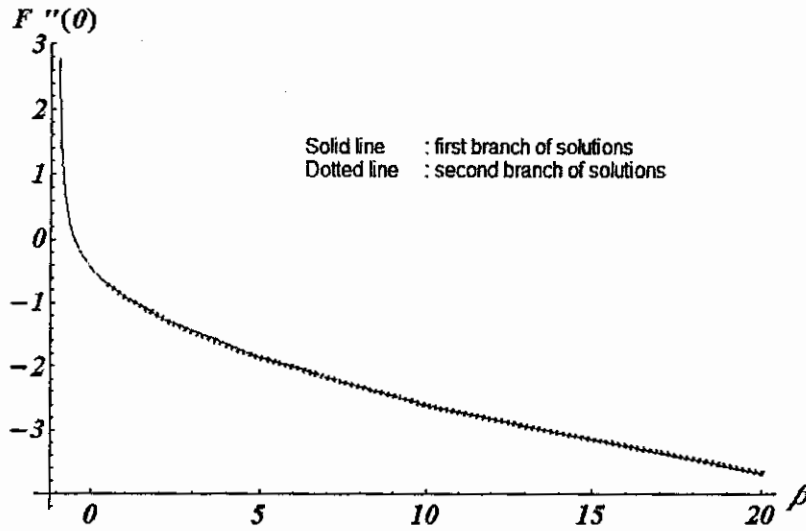
Fig. 2.5: Comparison of $F''(0)$ of the two branches of solutions of the boundary layer flows over a stretched wall. The difference of solutions of the two branches is not visible, because it is very small, as mentioned in main text.

Recently, Pop and Na [21] reported multiple solutions for MHD flows over a stretched permeable surface. Zaturska and Banks [5] found multiple solutions for Blasius boundary-layer flows. Magyari et al. [23] found multiple solutions of boundary-layer flows over a moving plane surface in a special case. In this chapter we assume that the solutions tend to zero exponentially at infinity. However, Magyari et al. [24] found that, when $\beta = 1/2$, Eqs.(2.5) and (2.6) have an infinite number of solutions with algebraic asymptotic property at infinity. It seems that the boundary-layer flows might have multiple solutions in general, and thus further investigations are necessary. And the homotopy analysis method provides us with a useful analytic tool for this purpose.

41

Chapter 3

Mixed convection and mass transfer in the stagnation point flow of second grade fluid adjacent to vertical surface

3.1 Introduction

Here, the influence of mass transfer on the stagnation point flow adjacent to a vertical surface with mixed convection is seen. The fluid is incompressible and viscoelastic. Infact this work is generalization of research presented by Hayat et al. [36] in the regime of mass transfer. Analysis with first order chemical reaction is presented. Homotopy analysis method is used to construct the solution of the mixed convection and mass transfer in two-dimensional stagnation point flows of second grade fluid around the heated surfaces for the case when the wall temperature varies linearly with the distance from the stagnation point. The two dimensional boundary layer equation governing the flow, thermal field and concentration fields are reduced to three nonlinear ordinary differential equation by using the set of similarity transformation. The solution of these equations are obtained in the buoyancy assisting and opposing regions. It is observed that, similar to the Newtonian flow case, a reverse flow regions develops for the

42

buoyancy opposing flow region. The influences of secondary parameters on the velocity, thermal and concentration fields are discussed in detail.

3.2   Basic equations

Let us consider a second grade fluid of uniform ambient temperature T_∞ and mass concentration C_∞ is flowing normal to the a heated vertical surface as shown in Fig. 3.1. It is further assumed that the free stream velocity of fluid is U_∞ at a large distance from the vertical plate. $T_w(x)$ be the temperature of the heated plate which obeys $T_w(x) > T_\infty$. The flow in the neighborhood of the stagnation line (x–axes) has the same characteristic irrespective of the shape of body. This flow is often referred to as a Hiemenz flow [35].
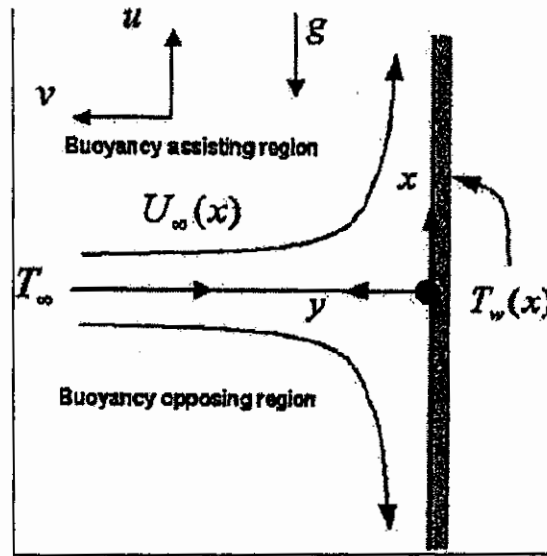
Fig. 3.1: Physical model and coordinate system.

In the absence of viscous dissipation and heat generation, under the Bounsinesq approximation, boundary layer equation steady state flow condition is given as

$$\frac{\partial u}{\partial x} + \frac{\partial v}{\partial y} = 0, \tag{3.1}$$

43

$$u\frac{\partial u}{\partial x} + v\frac{\partial u}{\partial y} = U\frac{\partial U}{\partial x} + v\frac{\partial^2 u}{\partial y^2} + k_0\left(u\frac{\partial^3 u}{\partial x\partial y^2} + \frac{\partial u}{\partial x}\frac{\partial^2 u}{\partial y^2} + \frac{\partial u}{\partial y}\frac{\partial^2 v}{\partial y^2} + v\frac{\partial^3 u}{\partial y^3}\right) \pm g\beta(T - T_\infty), \quad (3.2)$$

$$u\frac{\partial T}{\partial x} + v\frac{\partial T}{\partial y} = \alpha\frac{\partial^2 T}{\partial y^2}, \quad (3.3)$$

$$u\frac{\partial C}{\partial x} + v\frac{\partial C}{\partial y} = D\frac{\partial^2 C}{\partial y^2} - k_1 C, \quad (3.4)$$

subject to the boundary conditions

$$\left.\begin{array}{l} u = 0, \quad v = 0, \quad T = T_w(x), \quad C(x,y) = C_w \quad at \quad y = 0 \\[2mm] u \rightarrow U_\infty(x), \quad \frac{\partial u}{\partial y} \rightarrow 0, \quad T \rightarrow T_\infty, \quad C(x,y) \rightarrow C_\infty \ as \ y \rightarrow \infty \end{array}\right\}, \quad (3.5)$$

where C_w be the concentration at the sheet surface, x and y are Cartesian coordinates along and normal to the plate, respectively, u and v are the velocity components along x and $y-$axes, respectively, v be the kinematic viscosity, T be the temperature, g be the acceleration due to gravity, β be the thermal expansion coefficient, α be the thermal diffusibility and k_0 be the viscoelastic parameter and a and b are the positive constants. Furthermore, +ve and -ve sign indicated in Eq. (3.2) correspond to assisting and opposing flow respectively.

We look for a solution of Eqs. (3.1) − (3.4) of the form

$$\left.\begin{array}{l} \eta = \sqrt{\frac{a}{v}}y, \quad u = axf'(\eta), \quad v = -\sqrt{av}f(\eta), \\[2mm] \theta(\eta) = (T - T_\infty) \,/\, (T_w - T_\infty), \quad \phi(\eta) = (C - C_\infty) \,/\, (C_w - C_\infty) \end{array}\right\}. \quad (3.6)$$

After introducing the above transformation Eqs.(3.2) − (3.4) reduced to the following ordinary differential equations

$$f''' + f f'' - f'^2 + 1 \pm \lambda\,\theta - K(f''^2 - 2\,f\,f''' + f\,f^{iv}) = 0, \quad (3.7)$$

$$\theta'' + \Pr(f\,\theta' - f'\theta) = 0, \quad (3.8)$$

44

$$\phi'' + Sc \ (f \ \phi' - \delta \ \phi) = 0, \tag{3.9}$$

and the boundary conditions Eq. (3.5) becomes

$$\left. \begin{array}{l} f(0) = f'(0) = 0, \quad \theta(0) = 1, \quad \phi(0) = 1 \\ f'(\infty) = 1, \quad f''(\infty) = 0, \quad \theta(\infty) = 0, \quad \phi(\infty) = 0, \end{array} \right\}. \tag{3.10}$$

Where prime denotes the differentiation with respect to η and $\lambda \geq 0$ is the constant mixed convection parameter, $K \geq 0$ is the dimensionless viscoelastic parameter and Pr is the Prandtl number, Sc is the Schmidt number and δ is a chemical reaction which are defined as

$$\lambda = \frac{g\beta b}{a^2} = \frac{g\beta(T_w - T_\infty)x^2 \ / \ v^3}{U_\infty x^2 / \ v^2} = \frac{Gr_x}{Re_x^2}, \quad K = \frac{k_0 a}{\rho}, \quad Sc = \frac{v}{D}, \quad \delta = \frac{k_1}{c}, \tag{3.11}$$

with $Gr_x = g\beta(T_w - T_\infty)x^2 \ / \ v^3$ being the local Grashof number, $Re_x^2 = U_\infty x^2 / \ v^2$ is the local Reynolds number and ρ is the density of the fluid. Physical quantities of interest are defined as

$$C_f = \frac{\tau_w}{\rho U_\infty^2}, \qquad Nu_x = \frac{xq_w}{\alpha(T_w - T_\infty)}, \qquad \phi'(0) = \left(\frac{\partial \phi}{\partial y}\right)_{y=0}, \tag{3.12}$$

where τ_w and q_w are the wall friction and the heat transfer from the plate, which are given by

$$\left. \begin{array}{l} \tau_w = \mu \left(\frac{\partial u}{\partial y}\right)_{y=0} + k_0 \left(u\frac{\partial^2 u}{\partial x \partial y} + v\frac{\partial^2 u}{\partial y^2} - 2\frac{\partial u}{\partial y}\frac{\partial v}{\partial y}\right)_{y=0}, \\ q_w = -k \left(\frac{\partial T}{\partial y}\right)_{y=0}, \end{array} \right\}. \tag{3.13}$$

Using variables (3.7), we get

$$\left. \begin{array}{c} Re_x^{1/2} C_f = (f'' + K(3f'f'' - f f''))_{\eta=0} = f''(0) \\ Re_x^{-1/2} Nu_x = -\theta'(0) \\ \phi'(0) = \left(\frac{\partial \phi}{\partial y}\right)_{y=0} \end{array} \right\}, \tag{3.14}$$

In order to obtain the solution of Eqs. (3.7) − (3.10), Homotopy analysis method is employed as follows.

3.3 Solution by homotopy analysis method (HAM)

The initial approximations of $f(\eta), \theta(\eta)$ and $\phi(\eta)$ and the auxiliary linear operators $\mathcal{L}_1, \mathcal{L}_2$ and $\mathcal{L}_3$ are assumed as

$$\left. \begin{array}{l} f_0(\eta) = \eta - 1 + \exp(-\eta) \\ \theta_0(\eta) = \exp(-\eta) \\ \phi_0(\eta) = \exp(-\eta) \end{array} \right\}, \tag{3.15}$$

$$\left. \begin{array}{l} \mathcal{L}_1(f) = \dfrac{d^3 f}{d\eta^3} - \dfrac{df}{d\eta} \\[2mm] \mathcal{L}_2(\theta) = \dfrac{d^2 \theta}{d\eta^2} - \theta \\[2mm] \mathcal{L}_3(\phi) = \dfrac{d^2 \phi}{d\eta^2} - \phi \end{array} \right\}, \tag{3.16}$$

which satisfy the following properties

$$\left. \begin{array}{l} \mathcal{L}_1[C_1 + C_2 \exp(\eta) + C_3 \exp(-\eta)] = 0 \\ \mathcal{L}_2[C_4 \exp(\eta) + C_5 \exp(-\eta)] = 0 \\ \mathcal{L}_3[C_6 \exp(\eta) + C_7 \exp(-\eta)] = 0 \end{array} \right\}, \tag{3.17}$$

in which C_i, $i = 1-7$ are arbitrary constants, $p \in (0,1)$ and $\hbar_1, \hbar_2,$ and $\hbar_3$ indicate the embedding and non-zero auxiliary parameters, respectively. The zeroth-order deformation problems are of the following form

$$(1-p)\mathcal{L}_1[\widehat{f}(\eta;p) - f_0(\eta)] = p\hbar_1 H_1(\eta)\mathcal{N}_1[\widehat{f}(\eta;p)] \tag{3.18}$$

$$\widehat{f}(0;p) = 0, \qquad \widehat{f}\,'(0;p) = 0, \qquad \widehat{f}\,'(\infty;p) = 1 \tag{3.19}$$

$$(1-p)\mathcal{L}_2[\widehat{\theta}(\eta;p) - \theta_0(\eta)] = p\hbar_2 H_2(\eta)\mathcal{N}_2[\widehat{\theta}(\eta;p), \widehat{f}(\eta;p)] \tag{3.20}$$

$$\widehat{\theta}(0;p) = 1, \qquad \widehat{\theta}\,(\infty;p) = 0, \tag{3.21}$$

$$(1-p)\mathcal{L}_3[\widehat{\phi}(\eta;p) - \phi_0(\eta)] = p\hbar_3 H_3(\eta)\mathcal{N}_3[\widehat{\phi}(\eta;p), \widehat{f}(\eta;p)], \qquad (3.22)$$

$$\widehat{\phi}(0;p) = 1, \qquad \widehat{\phi}\ (\text{co};p) = 0, \qquad (3.23)$$

the non-linear operators $\mathcal{N}_1, \mathcal{N}_2$ and $\mathcal{N}_3$ are defined by

$$\left.\begin{aligned}
\mathcal{N}_1[\widehat{f}(\eta;p)] &= \frac{\partial^3 \widehat{f}(\eta;p)}{\partial\eta^3} + \widehat{f}(\eta;p)\frac{\partial^2 \widehat{f}(\eta;p)}{\partial\eta^2} - \left(\frac{\partial \widehat{f}(\eta;p)}{\partial\eta}\right)^2 + 1 \pm \lambda\widehat{\theta}(\eta;p) \\
&\quad -K\left(\left(\frac{\partial^2 \widehat{f}(\eta;p)}{\partial\eta^2}\right)^2 - 2\frac{\partial \widehat{f}(\eta;p)}{\partial\eta}\frac{\partial^3 \widehat{f}(\eta;p)}{\partial\eta^3} + \widehat{f}(\eta;p)\frac{\partial^4 \widehat{f}(\eta;p)}{\partial\eta^4}\right) \\
\mathcal{N}_2[\widehat{\theta}(\eta;p), \widehat{f}(\eta;p)] &= \frac{\partial^2\widehat{\theta}(\eta;p)}{\partial\eta^2} + \Pr\left(\widehat{f}(\eta;p)\frac{\partial\widehat{\theta}(\eta;p)}{\partial\eta} - \frac{\partial \widehat{f}(\eta;p)}{\partial\eta}\widehat{\theta}(\eta;p)\right) \\
\mathcal{N}_3[\widehat{\phi}(\eta;p), \widehat{f}(\eta;p)] &= \frac{\partial^2\widehat{\phi}(\eta;p)}{\partial\eta^2} + Sc\left(\widehat{f}(\eta;p)\frac{\partial\widehat{\phi}(\eta;p)}{\partial\eta} - \delta\ \widehat{\phi}(\eta;p)\right)
\end{aligned}\right\} \qquad (3.24)$$

and $H_1(\eta), H_2(\eta)$ and $H_3(\eta)$ are the base functions. For the present flow problem we consider

$$H_1(\eta) = \exp(-\eta), \qquad H_2(\eta) = 1\ = H_3(\eta).$$

Obviously for $p = 0$ and $p = 1$ we have

$$\left.\begin{aligned}
\widehat{f}(\eta;0) &= f_0(\eta), & \widehat{f}(\eta;1) &= f\ (\eta) \\
\widehat{\theta}(\eta;0) &= \theta_0(\eta), & \widehat{\theta}(\eta;1) &= \theta\ (\eta) \\
\widehat{\phi}(\eta;0) &= \phi_0(\eta), & \widehat{\phi}(\eta;1) &= \phi\ (\eta)
\end{aligned}\right\}. \qquad (3.25)$$

As p increases from 0 to 1, $\widehat{f}(\eta;p)$, $\widehat{\theta}(\eta;p)$ and $\widehat{\phi}(\eta;p)$ vary from its initial approximations $f_0(\eta)$, $\theta_0(\eta)$ and $\phi_0(\eta)$ to the exact solution $f\ (\eta)$, $\theta\ (\eta)$ and $\phi(\eta)$. Due to Taylor's theorem

47

$$
\left.\begin{aligned}
\widehat{f}(\eta; p) &= f_0(\eta) + \sum_{m=1}^{\infty} f_m(\eta)\, p^m \\
\widehat{\theta}(\eta; p) &= \theta_0(\eta) + \sum_{m=1}^{\infty} \theta_m(\eta)\, p^m \\
\widehat{\phi}(\eta; p) &= \phi_0(\eta) + \sum_{m=1}^{\infty} \phi_m(\eta)\, p^m
\end{aligned}\right\},
\tag{3.26}
$$

$$
\left.\begin{aligned}
f_m(\eta) &= \frac{1}{m!} \frac{\partial^m \widehat{f}(\eta; p)}{\partial p^m}\Big|_{p=0} \\
\theta_m(\eta) &= \frac{1}{m!} \frac{\partial^m \widehat{\theta}(\eta; p)}{\partial p^m}\Big|_{p=0} \\
\phi_m(\eta) &= \frac{1}{m!} \frac{\partial^m \widehat{\phi}(\eta; p)}{\partial p^m}\Big|_{p=0}
\end{aligned}\right\},
\tag{3.27}
$$

where convergence of the series in Eqs. (3.26) is ensured by $\hbar_1, \hbar_2, and\ \hbar_3$. Assume that $\hbar_1, \hbar_2,$ and $\hbar_3$ are selected such that the series in Eqs. (3.37) $-$ (3.39) are convergent at $p = 1$, then due to Eqs. (3.25) one can write

$$
\left.\begin{aligned}
f(\eta) &= f_0(\eta) + \sum_{m=1}^{\infty} f_m(\eta) \\
\theta(\eta) &= \theta_0(\eta) + \sum_{m=1}^{\infty} \theta_m(\eta) \\
\phi(\eta) &= \phi_0(\eta) + \sum_{m=1}^{\infty} \phi_m(\eta)
\end{aligned}\right\}.
\tag{3.28}
$$

Differentiating the zeroth-order deformation equations (3.18), (3.20) and (3.22) m times with respect to p, dividing by $m!$, and finally setting $p = 0$, we get the following mth-order deformation problems

$$
\left.\begin{aligned}
\mathcal{L}_1[f_m(\eta) - \chi_m f_{m-1}(\eta)] &= \hbar_1 \mathcal{R}_m^f(\eta) \\
\mathcal{L}_2[\theta_m(\eta) - \chi_m \theta_{m-1}(\eta)] &= \hbar_2 \mathcal{R}_m^\theta(\eta) \\
\mathcal{L}_3[\phi_m(\eta) - \chi_m \phi_{m-1}(\eta)] &= \hbar_3 \mathcal{R}_m^\phi(\eta)
\end{aligned}\right\},
\tag{3.29}
$$

$$
\left.\begin{aligned}
f_m(0) = f'_m(0) = f'_m(\infty) &= 0 \\
\theta_m(0) = \theta_m(\infty) &= 0 \\
\phi_m(0) = \phi_m(\infty) &= 0
\end{aligned}\right\},
\tag{3.30}
$$

48

$$
\left.
\begin{aligned}
R_m^f(\eta) &= f'''_{m-1}(\eta) + (1 - \chi_m) \pm \lambda\theta_{m-1} + \sum_{k=0}^{m-1} \left[f_{m-1-k} f''_k - f'_{m-1-k} f'_k \right] \\
&\quad - K \sum_{k=0}^{m-1} \left[f''_{m-1-k} f''_k - 2f'_{m-1-k} f'''_k + f_{m-1-k} f_k^{iv} \right] \\
\mathcal{R}_m^\theta(\eta) &= \theta''(\eta) + \Pr \sum_{k=0}^{m-1} \left[\theta'_{m-1-k} f - \theta_{m-1-k} f'_k \right] \\
\mathcal{R}_m^\phi(\eta) &= \phi''(\eta) - Sc\, \delta\, \phi_{m-1} + Sc \sum_{k=0}^{m-1} \phi'_{m-1-k} f_k
\end{aligned}
\right\}, \qquad (3.31)
$$

where

$$
\chi_k = \begin{cases} 0, & k \le 1 \\ 1, & k > 1 \end{cases} \qquad (3.32)
$$

The series solution of Eqs. (3.29) up to first few order of approximations have been obtained by using symbolic software Mathematica.

3.4   Convergence of the HAM solution

The convergence and rate of approximation for the HAM solution of the series (3.28) are strongly dependent upon the auxiliary parameters $\hbar_1, \hbar_2$ and $\hbar_3$. Therefore one can choose the proper value of $\hbar_1, \hbar_2$ and $\hbar_3$ by plotting the $\hbar$-curves which ensure that the solution series (3.28) converge, as suggested by Liao [18]. For this purpose the $\hbar$-curves are plotted against 15th-order of approximation in Fig. 3.2 for both cases of assisting and opposing flows. Fig. 3.2 clearly depicts that the range for the admissible values of $\hbar_1, \hbar_2$ and $\hbar_3$ $-1.9 \le \hbar_1 \le -0.3$, $-1.8 \le \hbar_2 \le -0.3$ and $-2.5 \le \hbar_3 \le 0$. Obviously our calculations shows that the series (3.28) converges in the whole region of η when $\hbar_{1,2,3} = \hbar = -1$.
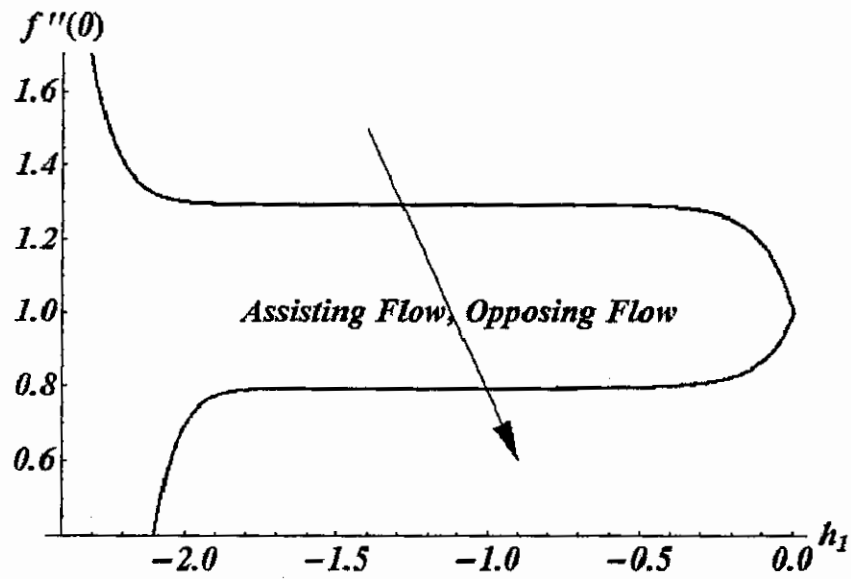
Fig. 3.2: $\hbar_1$-curves are plotted against the $15th - order$ of approximation for assisting and opposing flow for $f''(0)$ when $Pr = K = 0.2$, $Sc = \lambda = \delta = 0.5$.
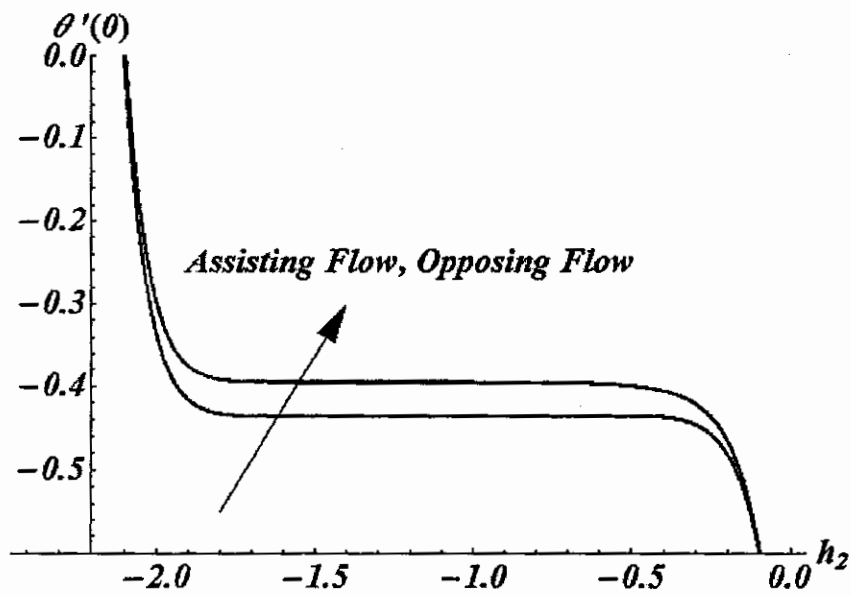

Fig. 3.3: $\hbar_2$-curves are plotted against the $15th - order$ of approximation for assisting and opposing flow for $\theta'(0)$ when $Pr = K = 0.2$, $Sc = \lambda = \delta = 0.5$.
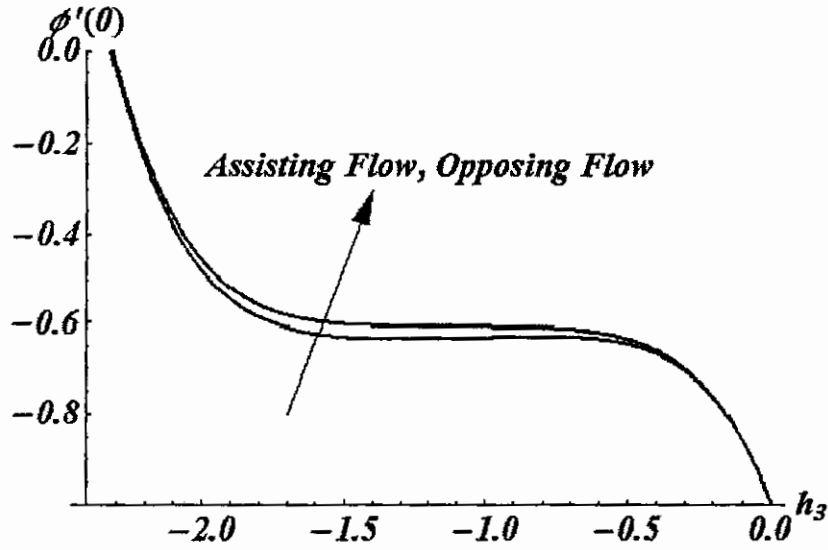
50

Fig. 3.4: $\hbar_3$ – curves are plotted against the $15th$ – $order$ of approximation for assisting and opposing flow for $\phi'(0)$ when $Pr = K = 0.2$, $Sc = \lambda = \delta = 0.5$.

Order of approximation	For assisting flow			For opposing flow		
	$f''(0)$	$-\theta'(0)$	$-\phi'(0)$	$f''(0)$	$-\theta'(0)$	$-\phi'(0)$
1	1.3733	0.2400	0.0946	0.8500	0.2875	0.0879
5	1.4133	0.3600	0.0925	0.8338	0.3285	0.0839
10	1.4190	0.3358	0.0926	0.8197	0.3019	0.0836
15	1.4190	0.3354	0.0927	0.8182	0.3006	0.0839
20	1.4190	0.3354	0.0927	0.8176	0.3002	0.0839
25	1.4190	0.3354	0.0927	0.8174	0.3001	0.0839
30	1.4190	0.3354	0.0927	0.8174	0.3001	0.0839

Table 1: Convergence of the missing initial condition $f''(0)$, $-\theta'(0)$ and $-\phi'(0)$ for assisting and opposing flows against different order of approximation.

3.5 Results and discussion
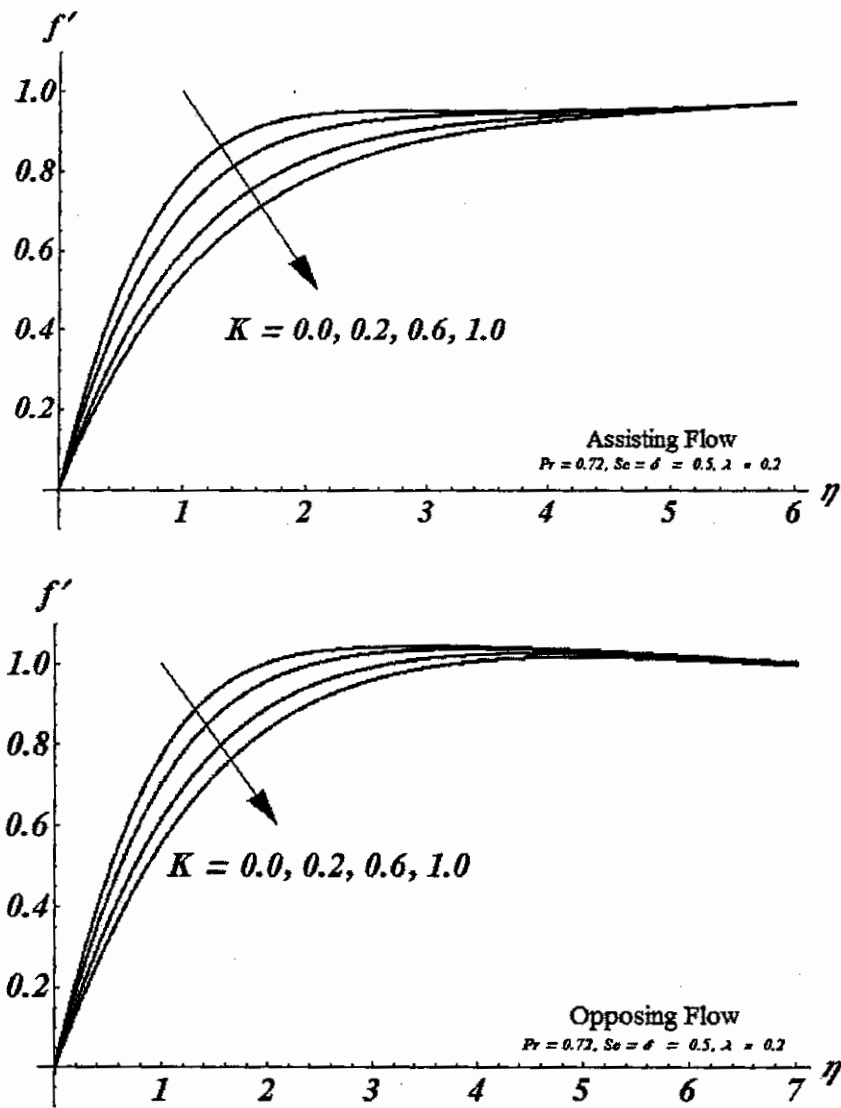
Fig. 3.5 (a,b): Effects of viscoelastic parameter K on the velocity f' for assisting and opposing flows.
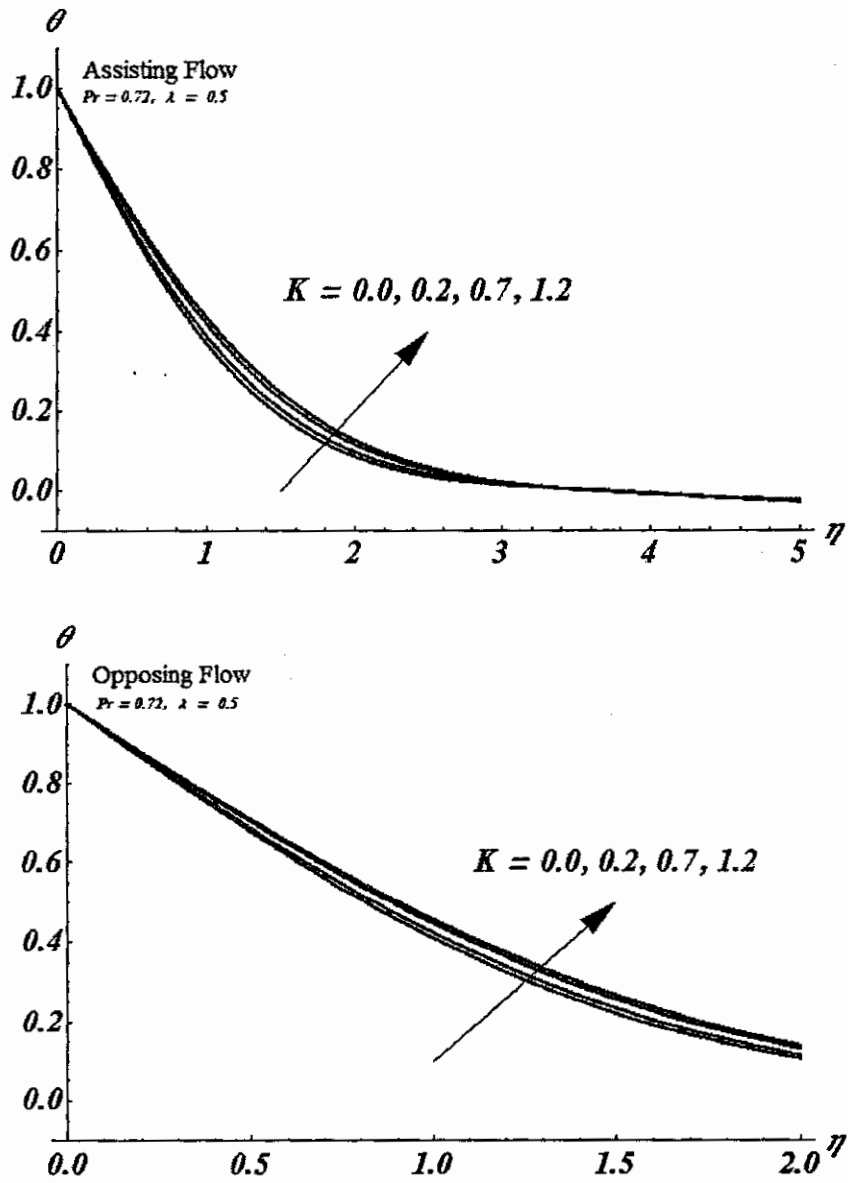
Fig. 3.6 (a,b): Effects of viscoelastic parameter K on the temperature θ for assisting and opposing flows.
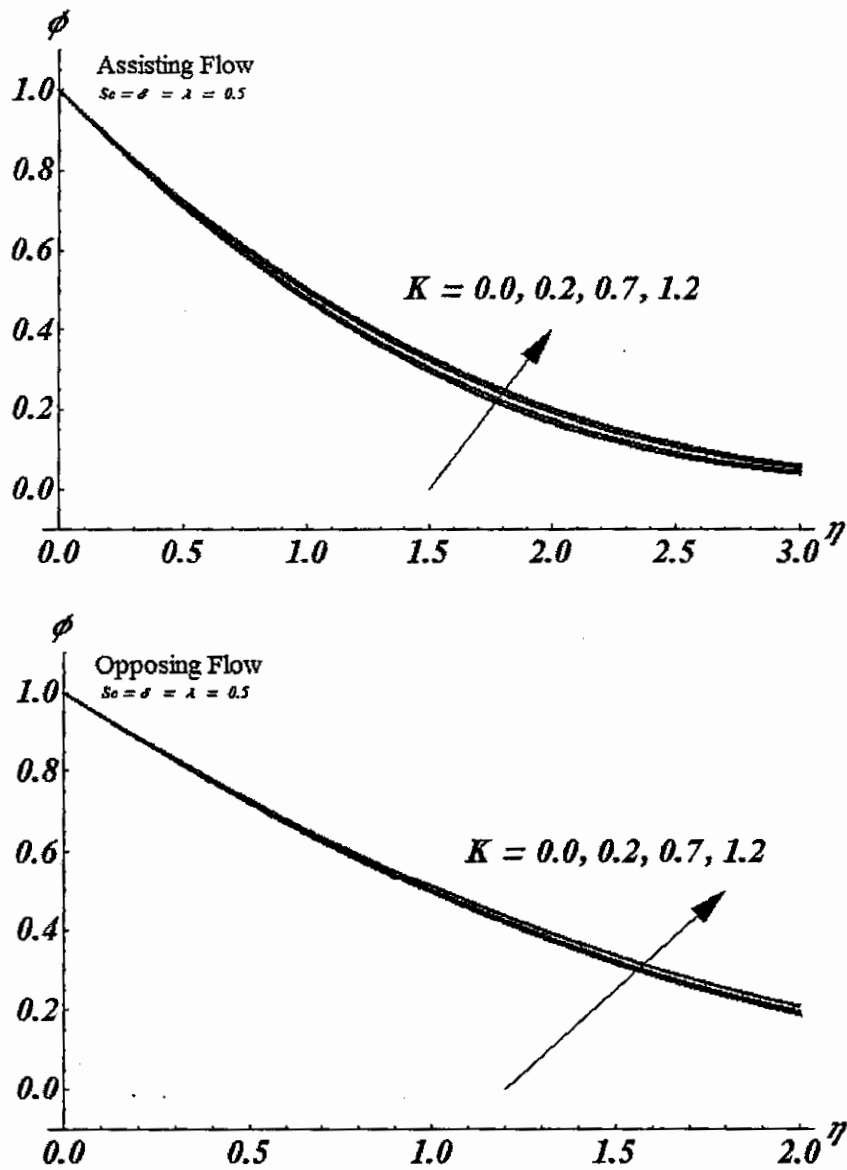
Fig. 3.7 (a,b): Effects of viscoelastic parameter K on the concentration field ϕ for assisting and opposing flows.
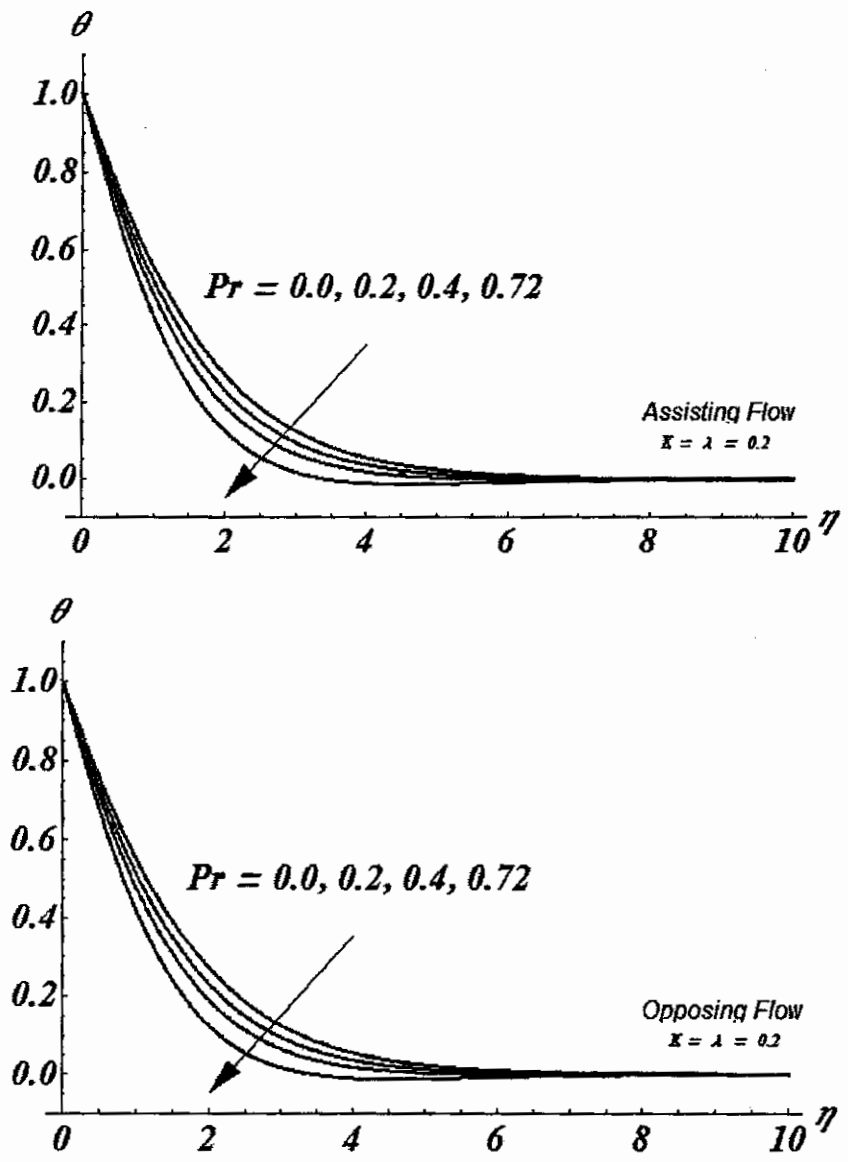
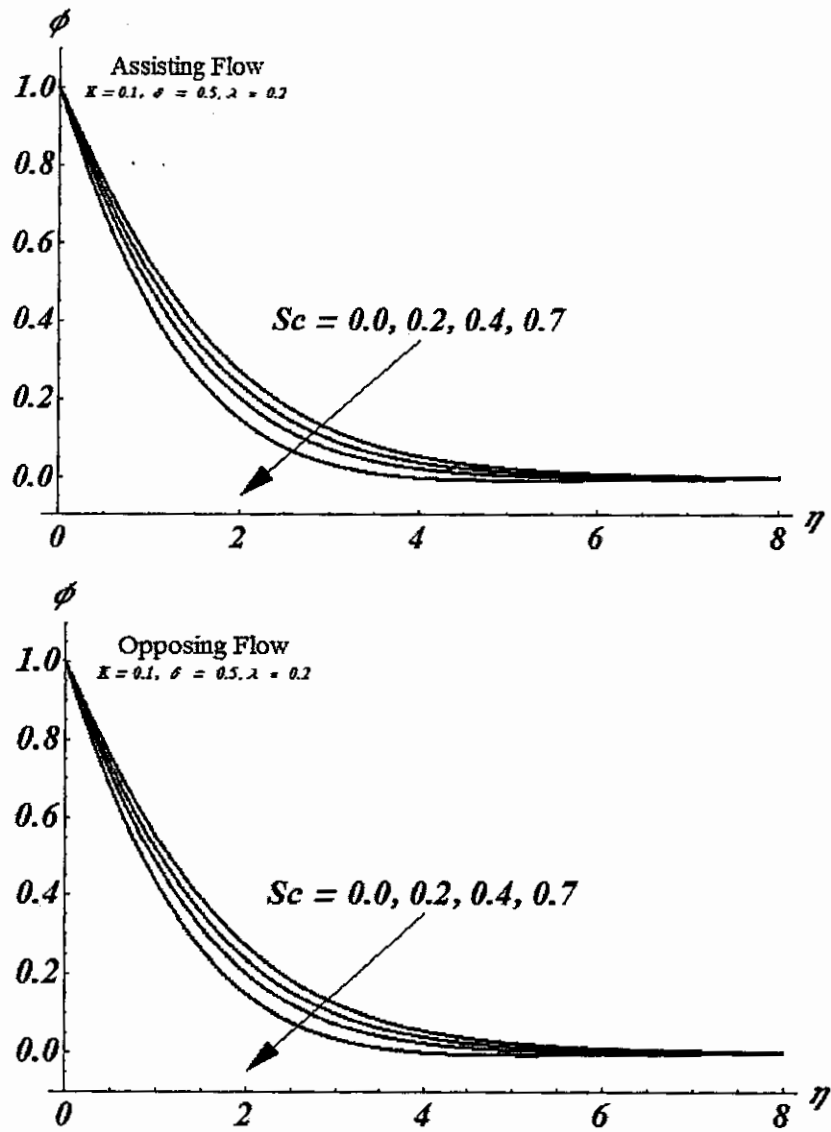Fig. 3.8 (a,b): Effects of Prandtl number Pr on the temperature θ for assisting and opposing flows.

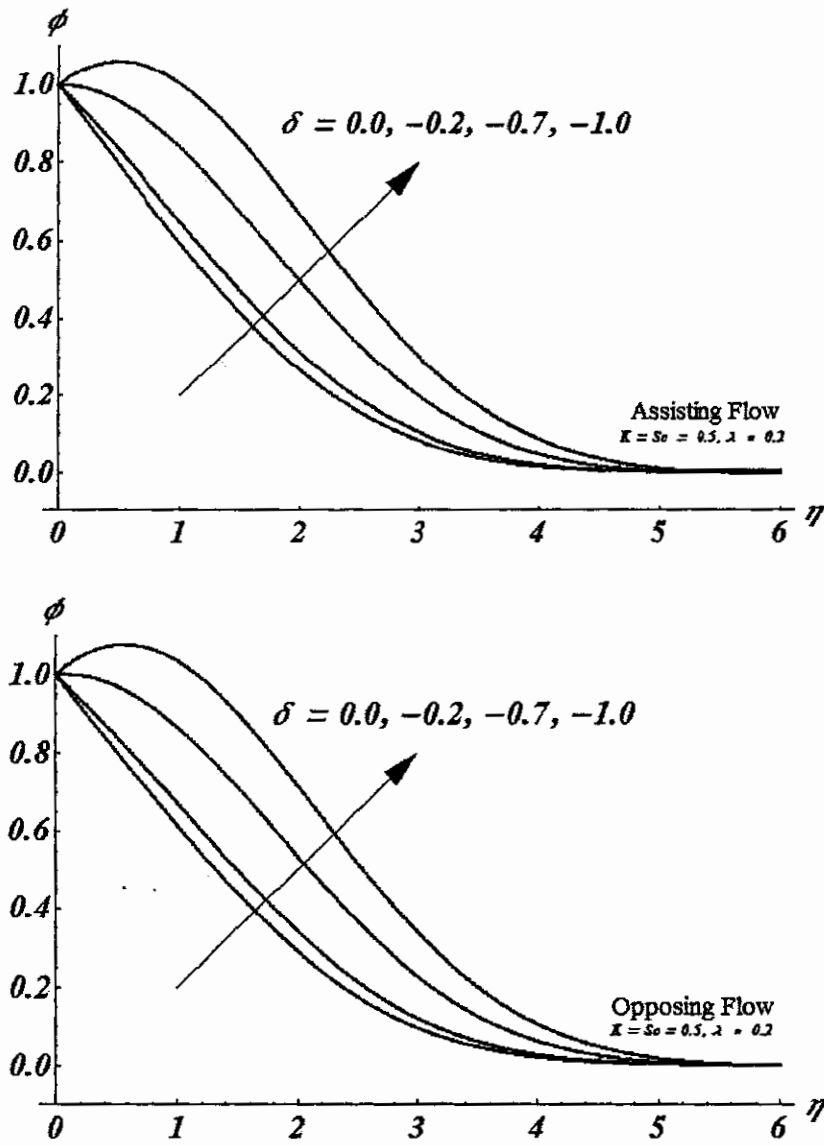Fig.3.9 (a,b): Effects of Schmidt parameter Sc on concentration field ϕ for assisting and opposing flows.

56

Fig. 3.10 (a,b): The variations of the generative chemical reaction parameter δ on the concentration field ϕ for assisting and opposing flows.
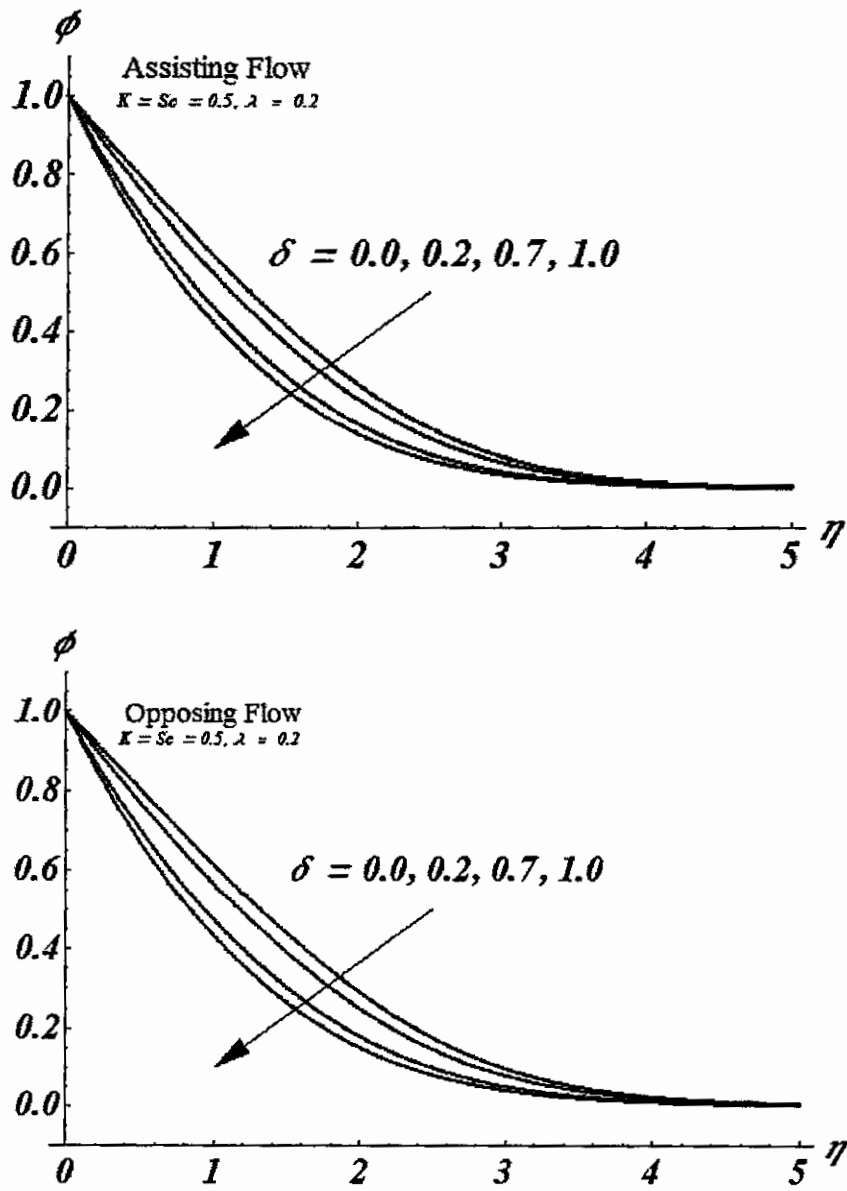
Fig. 3.11 (a,b): The variation of the destructive chemical reaction parameter δ on the concentration field ϕ for assisting and opposing flows.
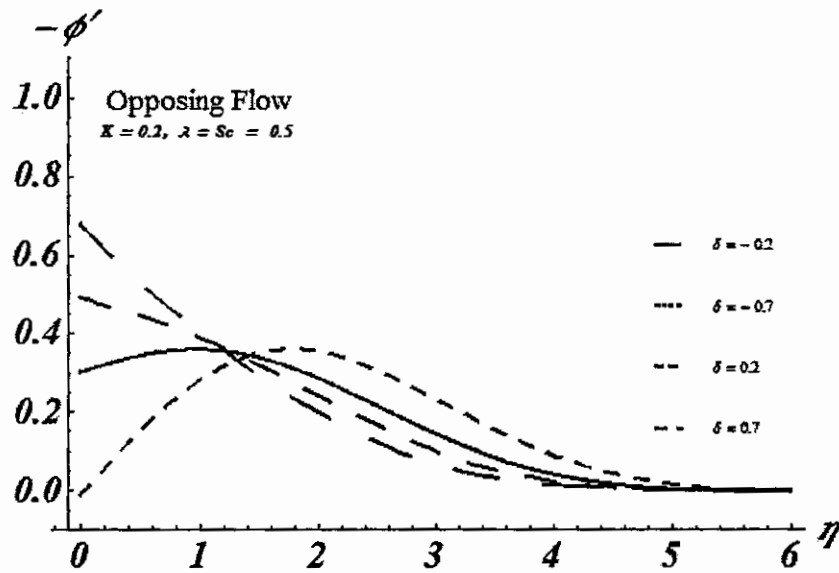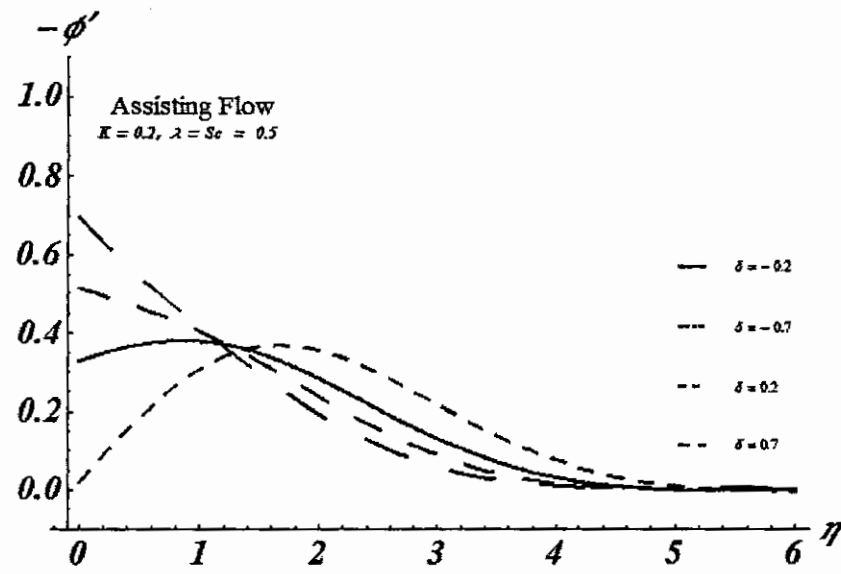
Fig. 3.12 (a,b): The variation of the chemical reaction parameter δ destructive / generative and on the grad of mass transfer $-\phi'(\eta)$ for assisting and opposing flows.
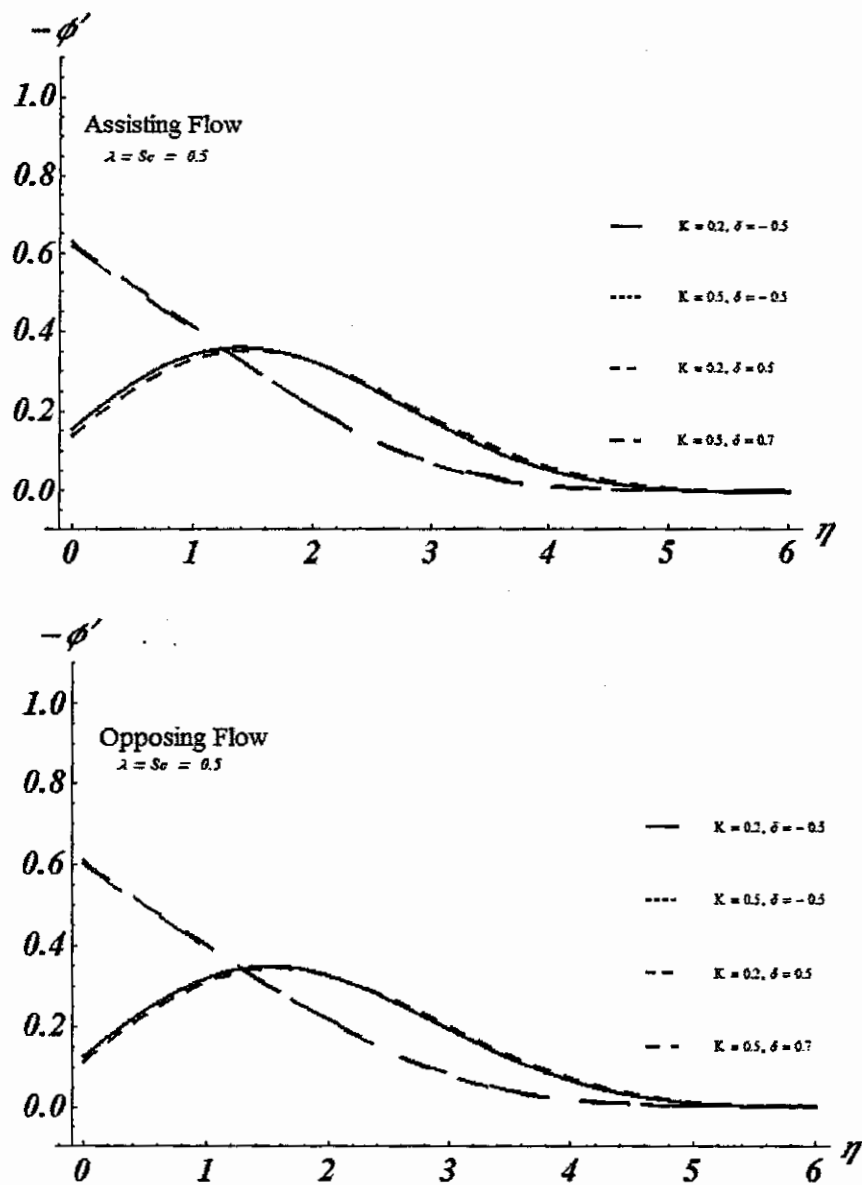
Fig. 3.13 (a,b): The variation of the viscoelastic K on the gradient of mass transfer $-\phi'(\eta)$ for destructive / generative chemical reaction for assisting and opposing flows.

In order to see the effects of some pertinent parameters involved in the system of differential equation like viscoelastic parameter K, the Prandtl number Pr, Schmidt number Sc, mixed

reaction parameter λ and chemical reaction parameter δ on velocity f', temperature θ and concentration field ϕ, Figs. 3.5-3.13 are drawn.

It is important to mention here that all the graphs are drawn against $10th - order$ solution obtained by the described homotopy analysis method. Furthermore, the graphs show the effects of assisting flows and opposing flows. Fig. 3.5(a,b) show the effects of viscoelastic parameter K on the velocity profile f' for assisting and opposing flows respectively. It is observed that velocity profile f' is decreasing function of K both for assisting and opposing flows. By increasing the viscoelasticity of the fluid, boundary layer thickness increases. For opposing flows it is seen that the reversal of the fluid flow occurs in presence of low viscoelastic effects of fluid and therefore the solution obtained for the opposing flow is not practical in nature as shown in Fig. 3.5 (b). Fig. 3.6 (a,b) depicts the variation on the temperature field θ due to K. The effects of K on the temperature field θ for assisting flow are comparatively dominant than of opposing flow. It can be seen that the temperature field θ increases due to increase in K. But its effects on thermal boundary layer thickness are very less bond in microscopic level, by increasing the viscoelasticity of the fluid, thermal boundary layer thickness increases both for assisting and opposing flows. Fig. 3.7(a,b) are drawn to show the effects of viscoelastic parameter on K on the concentration field ϕ. It is observed that the effects of K on the concentration field ϕ are very weak both for assisting and opposing flows. The effects of Pr on temperature field θ are shown in Fig. 3.8 (a,b). It is observed that by increasing the Prandtl number Pr, the temperature field and thermal boundary layer thickness decreases. The effects of Schimdt number on the concentration field are similar to that of Prandtl number Pr on temperature field both for assisting and opposing flows as shown in Fig. 3.9 (a,b). The effects of chemical reaction parameter δ on the concentration field ϕ are shown in Fig. 3.10 (a,b) and Fig. 3.11 (a,b). It is noted that $\delta < 0$ and $\delta > 0$ represent generative chemical reaction and destructive chemical reaction respectively. The effects of generative chemical reaction on the concentration field ϕ for assisting and opposing flows are very strong and concentration boundary layer thickness increases due to increase in generative chemical reaction. It is interesting to note here that the effects of destructive chemical reaction on concentration field are quite opposite to that of generative chemical reaction. The destructive chemical reaction can be used to reduce the concentration boundary layer thickness as shown in Fig. 3.11 (a,b). The effects of generative /

61

destructive chemical reaction on the gradient of mass transfer $-\phi'$ for the whole domain of η are shown in Fig. 3.12 (a,b). In both of these figures two curves represent generative chemical reaction and remaining represent destructive chemical reaction. It is observed that through both figures for generative chemical reaction, mass transfer gradient starts to increase upto almost 0.4 and after $\eta = 1.2$, it starts to decay to zero. But for destructive chemical reaction, mass gradient starts with same maximum number and continuously and smoothly decreases to zero. To see the variation in presence of viscoelasticity parameter K and generative / destructive chemical reaction δ on the concentration field, Fig. 3.13 (a,b) are shown. Fig. 3.7 (a,b) that the effects of viscoelastic parameter on concentration field are minimum. Similar effects are observed against mass gradient $\phi'(\eta)$ through Fig. 3.13 (a,b).

3.6 Concluding remarks

The main goal of this chapter is provide an analytical solution to a non-linear problem. For this purpose, HAM analysis has been used for mixed convection flow in a stagnation point in a second grade fluid. The simple and convenient expressions for velocity, temperature and mass transfer have been developed. The validity of the solutions for velocity, temperature and mass transfer has been explicitly discussed. The obtained series solutions confirm the power and ability of the HAM as an easy tool for computing the solution of non-linear problem. It is noted that the negative values of the temperature gradient and gradient of mass transfer provide an indication of the physical fact that the heat and mass transfer flows from the surface to the ambient fluid. The significance of the other parameters on the flow, temperature and mass transfer is high lighted. The analytic technique employed in this chapter can be used to other non-linear problems in the similar way.

Bibliography

[1] C. Sakiadis, Boundary Layer behavior on continuous solid surface, AIChE J. 7 (1961) 26-28.

[2] L.J. Crane, Flow past a stretching plate, ZAMP 21 (1970) 645-647.

[3] W.H.H. Banks, Similarity solutions of the boundary-layer equations for a stretching wall, J. Mec. Theor. Appl. 2 (1983) 375–392.

[4] L.J. Grubka and K.M. Bobba, Heat transfer characteristics of a continuous stretching surface with variable temperature, ASME J. Heat Transfer 107 (1985) 248–250.

[5] W.H.H. Banks and M.B. Zaturska, Eigen solutions in boundary layer flow adjacent to a stretching wall, IMA J. Appl. Math. 36 (1986) 263–273.

[6] L.E. Erickson, L.T. Fan and V.G. Fox, Heat and mass transfer on a moving continuous flat plate with suction or injection, Ind. Eng. Chem. 5 (1966) 19–25.

[7] P.S. Gupta and A.S. Gupta, Heat and mass transfer on a stretching sheet with suction or blowing, Can. J. Chem Eng. 55 (1977) 744–746.

[8] C.K. Chen and M.I. Char, Heat and mass transfer on a continuous stretching surface with suction or blowing, J. Math. Anal. Appl. 135 (1988) 568–580.

[9] M.E. Ali, Heat transfer characteristics of a continuous stretching surface, Wärm. Stoffübertr. 29 (1994) 227–234.

[10] M.A. Chaudhary, J.H. Merkin and I. Pop, Similarity solutions in the free convection boundary-layer flows adjacent to vertical permeable surfaces in porous media, Eur. J. Mech. B/Fluids 14 (1995) 217–237.

[11] E.M.A. Elbashbeshy, Heat transfer over a stretching surface with variable surface heat flux, J. Phys. D: Appl. Phys. 31 (1998) 1951–1954.

[12] E. Magyari and B. Keller, Exact solutions for self-similar boundary-layer flows induced by permeable stretching walls, Eur. J. Mech. B/Fluids 19 (2000) 109–122.

[13] S. Goldstein, On backward boundary layers and flow in converging passages, J. Fluid Mech. 21 (1965) 33–45.

[14] E. Magyari and B. Keller, Exact analytic solutions for free convection boundary layers on a heated vertical plate with laterial mass flux embedded in a saturated porous medium, Heat Mass Transfer 36 (2000) 109–116.

[15] S.J. Liao and I. Pop, Explicit analytic solution for similarity boundary layer equations, Int. J. Heat Mass Transfer 47 (1) (2004) 75–85.

[16] P. Cheng and W.J. Minkowycz, Flow about a vertical flat plate embedded in a porous medium with application to heat transfer from a disk, J. Geophys. Res. 82 (1977) 2040–2044.

[17] D.B. Ingham and S.N. Brown, Flow past a suddenly heated vertical plate in a porous medium, Proc. R. Soc. Lond. A 403 (1986) 51–80.

[18] S.J. Liao, Beyond Perturbation: Introduction to the Homotopy Analysis Method, Chapman and Hall/CRC Press, Boca Raton, 2003.

[19] S.J. Liao, On the analytic solution of magnetohydrodynamic flows of non-Newtonian fluids over a stretching sheet, J. Fluid Mech. 488 (2003) 189–212.

[20] S.J. Liao and K.F. Cheung, Homotopy analysis of nonlinear progressive waves in deep water, J. Eng. Math. 45 (2) (2003) 105–116.

[21] I. Pop and T.Y. Na, A note on flow over a stretching permeable surface, Mech. Res. Commun. 25 (1998) 263–269.

[22] M.B. Zaturska and W.H.H. Banks, A new solution branch of the Falkner–Skan equation, Acta Mech. 152 (2001) 197–201.

[23] E. Magyari, I. Pop and B. Keller, The missing similarity boundary-layer flow over a moving plane surface, Z. Angew. Math. Phys. 53 (2002) 782–793.

[24] E. Magyari, I. Pop and B. Keller, New analytic solutions of a well-known boundary value problem in fluid mechanics, Fluid Dynam. Res. 33 (2003) 313–317.

[25] S.J. Liao, A new branch of solutions of boundary-layer flows over an impermeable stretched plate, Int. J. Heat Mass Transfer 48 (2005) 2529–2539.

[26] B.D. Coleman and W. Noll, An approximate theorem for functionals, with applications in continuum mechanics, Arch. Rat. Mech. Anal. 56 (1974) 355–370.

[27] G. Pontrelli, Flow of a fluid of second grade over a stretching sheet, Int. J. Non-linear Mech. 30 (1995) 287–293.

[28] R.K. Bhatnagar, G. Gupta and K.R. Rajagopal, Flow of an Oldroyd-B fluid due to a stretching sheet in the presence of a free stream velocity, Int. J. Non-linear Mech. 30 (1995) 391–405.

[29] K. Sadeghy and M. Sharifi, Local similarity solution for the flow of a "second-grade" viscoelastic fluid above a moving plate, Int. J. Nonlinear Mech. 39 (2004) 1265–1273.

[30] D.W. Beard and K. Walters, Elastco-viscous boundary layer flows. Part I: two dimension flow near a stagnation point, Proc. Camb. Phil. Soc. 60 (1964) 667–674.

[31] V.K. Garg and K.R. Rajagopal, Stagnation-point flow of a non-Newtonian fluid, Mech. Res. Commun. 17 (1990) 415–421.

[32] R. Seshadri, N. Sreeshylan and G. Nat, Unsteady three-dimensional stagnation point flow of a viscoelastic fluid, Int. J. Eng. Sci. 35 (1997) 445–454.

65

[33] N. Ramachandran, T.S. Chen and B.F. Armaly, Mixed convection in stagnation flows adjacent to vertical surfaces, ASME J. Heat Transfer 110 (1988) 373–377.

[34] Y.Y. Lok, N. Amin, D. Campean and I. Pop, Steady mixed connection flow of a micropolar fluid near the stagnation point of a vertical surface, Int. J. Numer. Method. Heat Fluid Flow 15 (2005) 654–670.

[35] K. Hiemenz, Der Grenzschit an einem in den gleichförmigen Flüssigkeitsstrom einge-tauchten geraden Kreiszylinder, Dingl. Polytech J. 32 (1911) 321–410.

[36] T. Hayat, Z. Abbas and I. Pop, Mixed convection in the point flow adjacent to a vertical surface in a viscoelastic fluid, Int. J. Heat Mass Transfer 51 (2008) 3200-3206.